Downloaded from orbit.dtu.dk on: May 05, 2023

DTU Library

Linear accelerator radiography

Domanus, J.; Hansen, J.

Publication date:
1973

Document Version
Publisher's PDF, also known as Version of record

Link back to DTU Orbit

Citation (APA):
Domanus, J., & Hansen, J. (1973). *Linear accelerator radiography*. Risø National Laboratory. Risø-M No. 1599

General rights
Copyright and moral rights for the publications made accessible in the public portal are retained by the authors and/or other copyright owners and it is a condition of accessing publications that users recognise and abide by the legal requirements associated with these rights.

- Users may download and print one copy of any publication from the public portal for the purpose of private study or research.
- You may not further distribute the material or use it for any profit-making activity or commercial gain
- You may freely distribute the URL identifying the publication in the public portal

If you believe that this document breaches copyright please contact us providing details, and we will remove access to the work immediately and investigate your claim.

A. E. K. Risø

Risø - M - 1500

Risø - M - 1599

Title and author(s)

LINEAR ACCELERATOR RADIOGRAPHY

by

J. Domanus

and

Johnny Hansen

Date June 1973

Department or group

Metallurgy Dept.

Group's own registration number(s)

A-173

30 pages + 12 tables + 68 illustrations

Abstract

A description is given of the Risø lo MeV linear accelerator, which was used for radiography of steel (5o to 25o mm thick). Different X-ray film and intensifying screen combinations were tested and characteristic curves and exposure charts were computed. X-ray film speed and contrast were calculated.

Radiographic image contrast and quality were investigated and the best combination of X-ray film and screen was chosen.

Conclusions were drawn about the possibility of using the Risø accelerator for industrial radiography.

Copies to

Prof. A.R. Mackintosh
Dr. F. Juul
Dr. C.F. Jacobsen
M. Møller-Madsen
Metallurgy Dept. (4o)
Accelerator Dept. (5)

Abstract to

**Available on request from the Library of the Danish Atomic Energy Commission (Atomenergikommissionens Bibliotek), Risø, Roskilde, Denmark.
Telephone: (03) 35 51 01, ext. 334, telex:** 43116

Fi 25-204

ISBN 87 550 0197 1

LINEAR ACCELERATOR RADIOGRAPHY

by

J. Domanus

Elsinore Shipbuilding and Engineering Co., Ltd., Helsingør

and

Metallurgy Department, Danish Atomic Energy Commission,
Research Establishment Risø

and

Johnny Hansen

Accelerator Department, Danish Atomic Energy Commission,
Research Establishment Risø

March 1973

Work performed under contract between the Elsinore Shipbuilding and Engineering Co., Ltd. and the Metallurgy Department of the Danish Atomic Energy Commission, Research Establishment Risø.

CONTENTS

FIGURES

TABLES

1. INTRODUCTION

Since 1960 a 10 MeV Varian Model V-7700 linear accelerator has been used at Risø for radiation chemistry, dosimetry and sterilization purposes. It was decided to test the possibility of using this accelerator to perform radiography of thick steel castings.

The purpose of this investigation was to establish a correct exposure technique and to test the influence of different exposure factors on radiographic image quality.

In the first instance different X-ray film bands and intensifying screens were tested to determine characteristic curves and exposure charts for steel from 50 to 250 mm. From these curves, intensification factors for different film-screen-combinations were calculated.

Next, for different film-screen-combinations optimum radiographic image contrast and image quality were investigated. For that purpose a special slotted wedge penetrameter was used as well as ISO wire image quality indicators.

In the future other exposure factors (e.g. focus size, and focus film distance, and scattered radiation) will be investigated as well.

2. DESCRIPTION OF THE ACCELERATOR

2.1. The accelerator

The Risø accelerator is a two-section S-band electron linear accelerator with a maximum average output power of approx. 4.5 kW at 10 MeV. The linear accelerator is essentially a pulsed source of high energy electrons, with pulse lengths adjustable from 0.25 to 7 μs at peak pulse currents up to max. 320 mA. At a pulse length of 7 μs the maximum pulse current is 210 mA. The pulse repetition rate is stepwise variable from a single pulse to 300 pulses per second. The pulse shape is fairly rectangular with a rise time of the order of 0.1 μs.

The two accelerator guides, each 1 m long, are horizontally placed, and the electron beam can be directed through a straight-ahead window or down through a 90° bending magnet and a scanning system for irradiation of products carried on a conveyor. For the conversion of the electron beam into X-rays, a Bremsstrahlung converter is placed in front of the straight-ahead window in the beam centre line.

The electron beam inside the accelerator has a diameter of about 4 mm and a divergence of a few milliradians before it leaves the vacuum system. Scattering occurs at the 0.15 mm aluminium foil exit window, and the emerging beam is much more divergent. Within a distance of 50 cm from the exit window the electron beam in air has an almost linear divergence. At 50 cm its intensity decreases 50% from the centre to the edge of a 32 mm diameter field.

2.2. Beam parameters

To keep the radiation conditions as stable as possible beam parameters such as beam energy and average beam current must be controlled. In the straight-ahead mode of the accelerator there are no possibilities of continuous control of electron energy during irradiation. This means that after the initial warm-up period, the machine has to be checked a few times during the day because of further, gradual stabilisation or fading of various circuits.

The energy and current parameters determine the dose distribution throughout the sample as well as the average dose rate. To obtain reproducible radiation conditions from one irradiation period to another, the dose rate at a given position is measured by means of a dosimeter.

A relative measure of the electron energy is readily available as the accelerator is fitted with a bending magnet, and the magnet current needed to bend the beam through the 90° angle is proportional to the electron energy. Initial calibration[1] of the bending magnet has shown that it is possible to reproduce the main energy component with an accuracy of about 1%. Measurements of the current versus energy have shown that at 10 MeV 60% of the peak beam current is contained within an energy band of 10%.

An absolute measurement of the beam current can be made by having the electrons absorbed in a aluminium or graphite plate thick enough to absorb all the electrons entering it and by measuring the resulting current flowing to ground-potential. (The backscatter correction is less than 1% for aluminium at 10 MeV). A continuous measure of the peak pulse current can be made by means of a non-intercept monitor consisting of a toroidal pick-up coil, which is mounted around the beam centre line. The average current, determined from the peak pulse current, the pulse length and the pulse repetition rate, may change up to 15% in the course of one day if no readjustments are made. For the measurements described in this report frequent short and stops of the accelerator have been required, which may

implicate dose variations of no more than 10%.

2.3. Description of the Bremsstrahlung converter

The converter[2] consists of three sections: a tungsten plate, a cooling water slab, and a stainless steel backing plate. The X-ray photons are produced in the tungsten target by the stopping of the high energy electrons, while the water slab and the backing plate, which are located downstream from the tungsten disc, act as an electron filter as well as a hardener of the X-ray spectrum. Fig. 1 shows a calculated Bremsstrahlung spectrum for the converter.

As most of the beam power is stopped in the tungsten target, this causes a heavy thermal load, i.e. the permissible minimum beam diameter on the target is determined by the beam power and the mechanical properties of the material. From calculations on the converter target a minimum beam diameter of 20 mm was found necessary, lest the tungsten disc should not be damaged when the accelerator is operated at full output power. From measurements on the electron beam, showing the beam divergence in air, a distance of 20 cm from the accelerator exit window to the converter was chosen. At this distance the beam diameter containing 80% of the total electron current has increased to approximately 25 mm.

At a distance of 50 cm from the converter the forward angular intensity of the X-ray beam has been measured as absorbed dose rate by means of "Super-Fricke" dosimeters[3]. The results are shown in fig. 2 as the polar coordinates of the rate of the relative absorbed dose in water as a function of the angle. In the practical application, the dose rate in any given geometry has to be measured. The sample was positioned at a distance of 2 m from the converter in the beam centre line and the dose rate in water has been measured to 0.2 Mrad/h.

3. X-RAY FILMS AND INTENSIFYING SCREENS

Kodak Microtex, Agfa-Gevaert Structurix D2 and D4, and GAF 100, 200 and 400 X-ray films were used.

Metal intensifying screens: lead (0.15 + 0.25; 1 + 1 and 1.5 + 1.5 mm), copper (1 + 1 and 1.5 + 1.5 mm) as well as fluorometalic Kyokko SMP 101 and SMP 301 screens were used.

Table 1 shows what combinations of films and screens were used in the various stages of the investigation.

Table 1. X-ray films and intensifying screens. Investigation of:
C-characteristic curves
J-intensification factor
K-image contrast
Q-image quality

X-ray film	Investigated factor	Intensifying screens							
		No screens	Lead-mm			Copper-mm		Fluorometalic	
			0.15+0.25	1+1	1.5+1.5	1+1	1.5+1.5	SMP 101	SMP 301
Microtex	C J K Q	0	50-150	0;50-250 0 50-250 50-250	0 0	50-150 50-150 50-250	0 0 50-250	50-250 50-250 50-250	50-250 50-250 50-250
D2	C J K Q	0	50-150	0 0	0 0	50-150 50-150 50-150	0 0		
D4	C J K Q	0	50-150	0 0	0 0	50-150 50-150 50-150	0 0		
100	C J	0		0 0	0 0		0 0		
200	C J	0		0 0	0 0		0 0		
400	C J	0		0 0	0 0		0 0		

In the above table, the steel thickness ranges are given for which the investigation was performed (filtration of the X-ray beam).

4. EXPOSURE TECHNIQUE

The tungsten target was placed at a distance of 20 cm from the electron exit window of the accelerator, and X-ray films (in cassettes) were positioned at 2 m distance from the target. The distance between the film and a concrete wall of the accelerator cell was about 1 m.

In front of the film, steel plates (or steel penetrameters of different thicknesses from 50 to 250 mm) were placed.

The accelerator was run at 10 MeV with an electron current of 100 or 200 mA. The pulse length was 7 μs. The pulse repetition rate was either 37 or 300 pulses per second.

For short exposures (no steel filtration) 200 mA and 300 pps were used whereas for longer exposures 100 mA and 37 pps have to be applied to prevent overheating of the accelerator exit window. The end results are all relative to a 100 mA electron current.

Changes in exposure time were made by changing the number of pulses, keeping all other parameters constant.

5. EXPOSURE CONDITIONS

X-ray films in plastic cassettes, from which air was evacuated to ensure better contact between film and screens, were exposed either directly to X-radiation or through adequate filtration of steel.

For filtration purposes steel plates were used, ranging from 50 mm (one plate) up to 250 mm (five plates). Each plate (200 x 300 mm) was surrounded by additional masking steel plates: from the bottom and top by 100 x 500 mm plates, from the sides by 150 x 300 mm plates. Thus a steel block was formed having the surface of 500 x 500 mm and the thicknesses from 50 to 250 mm. All the elements used for the construction of such a block are seen on fig. 3. To keep the whole construction together a steel frame was used (at left of fig. 3). Fig. 4 shows the whole assembly.

In front of the steel block wire type image quality indicators (IQI) were placed during the investigation of the radiographic image quality.

6. SLOTTED STEEL WEDGE

For the investigation of radiographic contrast sensitivity a slotted steel wedge was used. The wedge was fabricated from a 250 mm thick steel plate, 1200 mm long. In this plate rectangular grooves were machined, having the following per cent depths: 0.25; 0.5; 1.0; 2.0 and 5.0. The grooves were 10 mm wide and spaced 20 mm from each other with a distance of 35 mm from the wedge edges (see fig. 5). At the top the wedge was 50 mm thick and at the bottom 250 mm thick. At a distance of 17.5 mm from the edge 11 holes (5 mm in diameter and 100 mm deep) were drilled at both sides of the wedge at intervals of 50 mm. These holes served as distance calibration points for the radiographs. Through the black spots, which these holes produced on the radiographs, parallel lines were drawn corresponding to the thickness of the step wedge (see table 2).

After machining the grooves in the steel wedge, the wedge was cut into four pieces each of a length of 300 mm (figs. 6 and 7). The thicknesses of the four steel wedges are: 50-100; 100-150; 150-200 and 200-250 mm.

Table 2. Thicknesses of the slotted steel wedge (mm)

Thickness range-mm		50-100	100-150	150-200	200-250
Calibration hole					
Distance from wedge edge-cm	No.				
2.5	1	54.2	104.2	154.2	204.2
5.0	2	58.3	108.3	158.3	208.3
7.5	3	62.5	112.5	162.5	212.5
10.0	4	66.6	116.6	166.6	216.6
12.5	5	70.8	170.8	170.8	220.8
15.0	6	75.0	125.0	175.0	225.0
17.5	7	79.1	129.1	179.1	229.1
20.0	8	83.3	133.3	183.3	233.3
22.5	9	87.5	137.5	187.5	237.5
25.0	10	91.6	141.6	191.6	241.6
27.5	11	95.8	145.8	195.8	245.8

Each slotted steel wedge was positioned between the masking steel plates as shown on figs. 8 and 9. The bottom and side masking plates had a thickness corresponding to the bottom thickness of the wedge, whereas the top masking plate had a thickness equal to the top thickness of the wedge.

The slotted steel wedge was used as a defectometer for the determination of the radiographic image contrast. The use of such a defectometer was previously described for X-rays[4] and for gammarays[5]. It was also used for a similar investigation in Co^{60} radiography[6] with satisfactory results.

7. CHARACTERISTIC CURVES OF X-RAY FILMS

Characteristic curves were computed for different X-ray film and intensifying screen combinations (as shown in table 1) and for exposures with and without different steel filtration.

7.1. Direct exposure

Kodak Microtex, Agfa-Gevaert Structurix D2 and D4, GAF 100, 200 and 400 X-ray films with and without 1.0 + 1.0 and 1.5 + 1.5 mm lead and 1.5 + 1.5 mm copper screens were directly exposed to the accelerator X-rays (without steel filtration) (table 1-marked o).

Film densities up to 5.0 were read on a "Quanta Log" Macbeth transmission densitometer. The characteristic curves were drawn for different exposures, given as number of pulses. They are presented on figs. 10 to 15. On those curves thicknesses of the intensifying screens are given ("o" means "no screens").

Figures 16 to 19 give a comparison of characteristic curves of various films for the same intensifying screens.

7.2. Exposure through steel

Kodak Microtex films with 0.15 + 0.25 and 1 + 1 mm Pb, 1 + 1 mm Cu metal intensifying screens and SMP 101 and SMP 301 fluorometalic screens as well as Agfa-Gevaert Structurix D2 and D4 films with 0.15 + 0.25 mm Pb and 1 + 1 mm Cu-screens were exposed through steel wedges of various thicknesses (see table 1). From the radiographs of steel wedges density readings were made at different wedge thicknesses (as shown in table 2), and

from these readings characteristic curves were computed as shown on figs. 2o to 28. On these figures wedge thickness ranges are marked, and for each range 11 curves are given. Each curve corresponds to the thickness specified in table 2 (first curve to the left corresponds to line No. 1, last curve to the right corresponds to line No. 11). Because of overlapping less than 11 curves are reproduced for a given thickness range. On some curves there is a lack of continuity and some curves are displaced in different pulse number regions. This was due to the fact that during a series of exposures of the wedge the required density range could not be reached and the exposures were repeated later. This was connected with another setting of the accelerator parameters and it was difficult to obtain exactly the same dose per pulse in the X-ray beam. Therefore, for the same number of pulses different doses of radiation were absorbed by the film (for explanation see section 2).

8. INTENSIFICATION FACTORS

From the characteristic curves shown on figs. 1o to 15 intensification factors for lead and copper screens were calculated (as the relation between number of pulses necessary to give the same film density for the film exposed with and without intensifying screens).

Table 3. gives the results of these calculations.

Table 3. Intensification factors

Film	Intensifying screens		
	1 + 1 mm Pb	1.5 + 1.5 mm Pb	1.5 + 1.5 mm Cu
Kodak Microtex	5.10	4.49	1.64
Strúrix D2	5.40	4.71	1.69
D4	5.01	3.46	1.83
GAF 100	5.97	5.89	2.11
200	5.13	3.92	3.39
400	4.29	3.56	2.00

In computing table 3 intensification factors were first calculated for the following densities: o.5; 1.o; 1.5; 2.o; 2.5; 3.o; 3.5 and 4.o. Next, for each film-screen-combination, mean values of intensification factors for all those densities were calculated; these values are given in table 3.

As can be seen, the best intensification is obtained with 1 + 1 mm lead screens. Copper screens give much poorer intensification than lead of the same thickness.

9. FILM SPEED AND CONTRAST

Speed and contrast of different X-ray film-and-screen combinations were determined using the American Standard Method for the Sensitometry of Industrial X-ray Films for Energies up to 3 Million Electron Volt.

9.1. Film speed

According to this standard X-ray film speed is determined for the density of 1.5 above the base and fog density. The speed of the film is taken as the reciprocal of exposure, measured in roentgens, necessary to produce a density of 1.5.

In the present investigation only relative film speed densities were determined and therefore they are given in arbitrary units.

Table 4. gives relative speeds (speed of Kodak Microtex film taken as 1.o) of X-ray films, calculated for direct exposures done without steel filtration.

Table 4. Relative film speeds (exposed without steel filtration)

Film	Intensifying screens			
	No screens	Lead screens		Copper screens
		1+1 mm	1.5+1.5 mm	1.5 + 1.5 mm
M	1.00	1.00	1.00	1.00
D2	0.44	0.46	0.46	0.45
D4	1.56	1.53	1.20	1.74
100	0.39	0.46	0.51	0.50
200	0.70	0.70	0.61	1.45
400	1.62	1.36	1.28	1.97
M	1.00	5.10	4.43	1.64
D2	0.44	2.37	2.07	0.74
D4	1.56	7.81	5.39	2.85
100	0.39	2.32	2.30	0.82
200	0.70	3.59	2.74	2.37
400	1.62	6.95	5.77	3.24

For X-ray films exposed through different thicknesses of steel relative speeds have been calculated for density 1.5 in the middle of each wedge thickness (i.e. behind 75, 125, 175 and 225 mm of steel). The results of these calculations are shown in table 5.

From tables 3 and 5, the following relative intensification factors can be computed in relation to films exposed with 1 + 1 mm Pb screens (relative intensification factor 1.0).

Table 5. Relative film speeds (exposed through steel)

Intensifying screens	Steel thickness mm	Film		
		M	D2	D4
0.15+0.25Pb	75	0.66	0.17	1.07
	125	1.33	0.35	2.60
1 + 1 Pb	75	1.0		
	125	1.0		
	175	1.0		
	225	1.0		
1 + 1 Cu	75	0.41	0.10	0.68
	125	0.85	0.24	1.30
SMP 101	75	1.55		
	125	1.44		
	175	1.66		
	225	2.00		
SMP 301	75	2.66		
	125	2.40		
	175	2.56		
	225	3.33		

Table 6. Relative intensification factors

Film	Steel filtration - mm					
	0		50-150		50-250	
	Intensifying screens					
	1.5+1.5Pb	1.5+1.5Cu	0.15+0.25Pb	1+1 Cu	SMP 101	SMP 301
Kodak Microtex	0.88	0.32	0.99	0.63	1.66	2.74
Structurix D2	0.87	0.31				
" D4	0.69	0.36				
GAF 100	0.86	0.35				
200	0.76	0.66				
400	0.83	0.46				

In the above table mean values of film speeds were taken from table 5 (for the whole range of steel filtration).

9.2. Film contrast

According to ASA standard PH 2.8[7] the average film gradient is defined as the slope of the straight line drawn on the characteristic curve between the points corresponding to densities of 0.5 and 2.5.

The average gradient = $\frac{2.0}{\log E_2 - \log E_1}$ where

E_2 is the exposure corresponding to a density of 2.5, E_1 is the exposure corresponding to a density of 0.5.

Following the above formula average gradients for different X-ray film and screen combinations were computed and are shown in table 7.

Table 7. Average gradients of X-ray films

Intensifying screens	Steel thickness mm	Film brand					
		Kodak Microtex	Structurix		GAF		
			D2	D4	100	200	400
0	0	6.94	5.39	6.66	7.24	5.83	6.89
0.15+0.25Pb	75	5.30	4.21	4.68			
	125	4.54	3.77	4.42			
1 + 1 Pb	0	6.94	6.33	7.60	6.73	5.68	5.97
	75	4.76					
	125	4.85					
	175	5.76					
	225	4.30					
1.5+1.5Pb	0	7.11	6.00	6.97	6.73	6.11	7.35
1 + 1 Cu	75	3.95	4.82	4.56			
	125	4.60	4.82	4.71			
1.5+1.5Cu	0	5.83	5.98	5.02	6.29	5.64	5.26
SMP 101	75	5.88					
	125	5.88					
	175	5.63					
	225	5.06					
SMP 301	75	5.61					
	125	5.46					
	175	5.66					
	225	4.70					

The average gradient was calculated for E_2 and E_1 corresponding to densities 3.5 and 1.5 as most of the characteristic curves did not have densities less than 0.5.

1o. ATTENUATION IN STEEL

Attenuation of X-ray radiation from the accelerator was measured using "Super-Fricke" dosimeters. For that purpose the same steel plates were used as shown on fig. 4. The attenuation curve obtained from these measurements is shown on fig. 29.

There per cent attenuation is given as well as the attenuation factor k (reciprocal of the attenuation).

11. RADIOGRAPHIC IMAGE CONTRAST

For X-ray films and intensifying screens and steel thickness ranges, shown in table 1, radiographs of a slotted steel wedge were made. For each slotted wedge (5o-1oo; 1oo-15o; 15o-2oo and 2oo-25o mm) films were exposed with different number of pulses so as to reach film densities between 2 and 3 at both ends of the wedge. All films were then developed in an automatic film processing machine and film densities (up to 5) were read on a "Quanta Log" Macbeth transmission densitometer.

The radiographs were read by two observers, and only such readings were taken into account where both observers could see the same slot on the radiograph. The radiograph of each slotted wedge was read along 11 lines, drawn through images of the holes drilled in the wedge. Thus it was possible to assess the radiographs at different wedge depths (all together 4 x 11 = 44 depths, as shown in table 2).

From the assessment of visibility of slots of different depth on wedge radiographs, diagrams were prepared, showing thickness ranges, in which the particular slots could be seen on the radiographs, in function of exposure (number of pulses) (similar to curves given in (4) and (5)). These diagrams are shown on figures 3o to 38. On these figures areas of visibility of the five slots of different per cent depth are given.

From these diagrams, the following conclusions can be drawn. The o.25% slot was sometimes visible only on Kodak Microtex film with 1 + 1 mm Pb screens in the range from 5o to 2oo mm of steel. The visibility of the deeper slots is given in table 8 for different steel thickness regions.

Table 8. Thickness regions in mm of Fe of slot visibility on radiographs

Film and Screen Combination	Per Cent Slot Depth			
	0.5	1	2	5
M 1+1 Pb	54-246	54-246	54-246	54-246
M SMP 101	54-229	54-241	54-246	54-246
M SMP 301	54-225	54-241	54-246	54-246
M 0.15+0.25 Pb	104-146	54-146	54-146	54-146
M 1+1 Cu	107-146	54-146	54-146	54-146
D2 0.15+0.25 Pb	104-146	54-146	54-146	54-146
D2 1+1 Cu	104-146	54-146	54-146	54-146
D4 0.15+0.25 Pb	104-141	54-146	54-146	54-146
D4 1+1 Cu	104-141	54-146	54-146	54-146

From the diagrams (figs. 3o to 38) one can see that for increasing slot depth the latitude of exposure increases for the same slot depth visibility.

Results quoted in table 8 cannot give a final answer to the question which X-ray film and screen combination will give the best radiographic image contrast. Therefore the radiographs of the slotted wedges were further investigated by means of a scanning densitometer (seen on fig. 39). Each radiograph was scanned along 11 lines on each radiograph (at different wedge thicknesses - see table 2) and densitometer readings were recorded by a paper chart recorder. From the results obtained during these transverse scans absolute and relative increases in film densities could be measured and calculated for different per cent depths of the slots. The results of the above are given in table 9.

From table 9 the following conclusions can be drawn. Kodak Microtex film with 1 + 1 mm Pb screens gives the best radiographic image contrast, especially in the region of greater steel thicknesses (above 15o mm), where the application of accelerator radiography presents most advantages. The fluorometalic intensifying screens give very good results (even better than lead screens) in the region up to 15o mm Fe. Above this thickness they are poorer than lead.

Table 9. Maximum density differences for different per cent slot depths

Film	Screens	mm Fe	5%		2%		1%		0.5%	
			D	ΔD	ΔD%	D	ΔD	ΔD%	D	ΔD	ΔD%	D	ΔD	ΔD%
M	1+1 Pb	50-100	1.07	0.05	5.01	1.12	0.023	2.06	2.14	0.03	1.40	1.43	0.01	0.73
		100-150	1.60	0.13	7.90	3.03	0.10	3.29	1.65	0.03	2.01	2.05	0.04	2.25
		150-100	2.00	0.19	9.64	2.10	0.09	4.32	2.14	0.05	2.21	1.52	0.02	1.50
		200-250	1.95	0.16	8.24	2.04	0.07	3.44	2.06	0.04	2.01	2.06	0.02	1.13
M	SMP	50-100	1.05	0.06	5.64	1.08	0.034	3.10	3.64	0.09	2.54	3.57	0.043	1.21
	101	100-150	1.90	0.15	8.15	1.09	0.035	3.24	2.02	0.05	2.40	1.06	0.012	1.10
		150-200	2.05	0.15	7.60	1.08	0.03	2.75	3.00	0.06	1.90	2.05	0.04	1.89
		200-250	1.98	0.128	6.47	2.02	0.04	2.29	1.08	0.02	1.78	2.00	0.015	0.77
M	SMP	50-100	1.03	0.06	6.51	2.14	0.056	2.61	2.14	0.05	2.22	2.08	0.031	1.48
	301	100-150	1.57	0.13	8.48	3.17	0.11	3.44	3.50	0.11	3.08	3.09	0.036	1.17
		150-200	1.88	0.15	7.89	3.77	0.115	3.06	3.82	0.046	1.22	1.46	0.015	1.06
		200-250	1.52	0.08	5.75	3.07	0.06	2.02	3.08	0.046	1.49	2.06	0.04	1.95
M	0.15 +	50-100	1.03	0.03	3.03	1.07	0.16	1.54	3.68	0.045	1.22	3.62	0.03	0.82
	0.25Pb	100-150	1.99	0.105	5.27	2.08	0.04	2.05	2.57	0.044	1.71	2.48	0.019	0.77
M	1+1 Cu	50-100	2.08	0.095	4.57	1.62	0.038	2.33	2.71	0.038	1.42	1.20	0.011	0.897
		100-150	2.85	0.205	7.19	2.96	0.088	2.94	2.47	0.043	1.72	1.04	0.01	0.99
D 2	0.15 +	50-100	2.25	0.09	3.99	1.76	0.033	1.87	1.77	0.02	1.10	2.37	0.017	0.69
	0.25 Pb	100-150	2.91	0.19	6.53	3.04	0.07	2.40	3.06	0.07	2.17	1.56	0.010	0.67
D 2	1+1 Cu	50-100	2.17	0.07	3.33	3.79	0.068	1.81	3.72	0.057	1.50	2.68	0.018	0.66
		100-150	1.22	0.086	6.99	1.24	0.042	3.44	1.24	0.029	2.30	1.21	0.019	1.77
D 4	0.15 +	50-100	2.17	0.08	3.78	1.27	0.021	1.63	2.21	0.02	0.94	3.26	0.017	0.51
	0.25 Pb	100-150	1.63	0.08	5.22	3.07	0.06	1.94	3.63	0.046	1.28	1.64	0.008	0.51
D 4	1+1 Cu	50-100	2.23	0.11	5.06	2.88	0.075	2.54	2.90	0.036	1.23	1.86	0.013	0.69
		100-150	1.10	0.09	8.51	1.10	0.035	3.21	2.54	0.05	1.98	2.50	0.016	0.63

Another advantage of the flourometalic screens is the shortening of exposure time. In comparison with the 1 + 1 mm Pb screens exposure can be cut down to 50% with SMP 101 and to 33% with SMP 301 screens.

12. RADIOGRAPHIC IMAGE QUALITY

The assessment of the radiographic image quality was done by the ISO wire IQI's. For that purpose steel wire 1ISO7 and 6ISO12 IQI's were used having the following wire diameters.

Table10. Wire diameters of the ISO IQI's

IQI	Wire number	1	2	3	4	5	6	7
1ISO7	Wire diameter-mm	3.20	2.50	2.00	1.60	1.25	1.00	0.80
IQI	Wire number	6	7	8	9	10	11	12
6ISO12	Wire diameter-mm	1.00	0.80	0.63	0.50	0.40	0.32	0.25

Fig. 40 gives the per cent IQI sensitivity for steel thicknesses from 50 to 250 mm for IQI's from table 10.

The above mentioned indicators were placed in front of the steel plates (on the source side) of different thicknesses, and wires of minimum diameter seen on the radiographs were read by two observers, and only such readings were taken into account where both observers could see the same wire.

The IQI sensitivity was checked several times using different X-ray film and screen combinations. During these checks different film densities were obtained. The results are shown on figs. 41 to 48.

Table 11 gives film densities obtained during these investigations.

Table 11. Film densities during radiographic image quality investigations

Steel thickness - mm			50	100	150	200	250
Film	Screens	Fig.No.					
GAF 100	1+1 Pb	41	1.86	1.82			
GAF 200							
GAF 400							
D 2			2.27	2.17	1.79	2.29	3.59
D 4			2.76	2.62	1.82	2.35	3.48
M			2.68	2.35	2.28	3.04	4.86
GAF 100	1+1 Pb	42	1.30	1.24	1.52	1.58	1.30
GAF 200							
GAF 400			1.32	1.34	1.59	1.48	1.34
D 2			1.25	1.19	0.95	0.77	0.91
D 4			3.22	2.84	2.74	2.41	2.42
M			1.40	1.33	1.48	1.38	1.36
GAF 100	1.5+1.5 Pb	43	1.75	1.50	1.50	1.55	1.80
GAF 200			1.45	1.45	1.75	2.00	1.80
GAF 400			1.80	1.80	1.65	1.80	2.20
D 2			1.80	2.00	2.00	2.15	2.50
D 4			2.15	1.95	2.15	2.40	2.30
M			1.75	1.95	1.9	2.20	2.40
GAF 100	1.5+1.5 Pb	44	1.96	1.96			
GAF 200							
GAF 400							
D 2			2.14	2.07	2.50	2.37	4.29
D 4			3.07	3.38	2.87	2.72	4.34
M			2.41	2.16	2.34	2.82	5.94

Table 11 continued

Steel thickness - mm			50	100	150	200	250
Film	Screens	Fig.No.					
GAF 100	1.5+1.5 Pb	45	1.30	1.38	1.50	1.65	1.08
GAF 200							
GAF 400			1.84	1.82	1.80	1.64	1.39
D 2			2.42	1.21	1.23	0.94	1.07
D 4			4.94	3.10	3.52	2.88	2.64
M			2.03	1.56	1.36	1.52	1.28
GAF 100	1.5+1.5 Pb	46	1.75	1.50	1.50	1.65	1.80
GAF 200			1.45	1.45	1.75	2.00	1.80
GAF 400			1.84	1.82	1.80	1.80	2.26
D 2			2.42	2.00	2.00	2.15	2.50
D 4			2.15	1.95	2.15	2.40	2.64
M			2.03	1.95	1.90	2.2	2.4
GAF 100	1.5+1.5 Cu	47	2.48	2.88	2.88	2.38	2.54
GAF 200			2.69	3.68	3.71	3.24	4.30
GAF 400			2.19	1.85	3.14	2.56	2.96
D 2			3.33	2.81	2.67	2.20	2.83
D 4			1.92	3.80	3.30	2.90	3.60
M			2.45	3.16	2.50	2.43	3.32
D 2	0.15+0.25Pb	48	4.38	4.12	4.47		
D 4			>5.00	4.38	4.72		
M			4.80	4.18	3.73	4.25	>5.00
M	1+1 Pb	48	3.50	3.16	2.58	2.42	2.75
	1.5+1.5 Pb		4.17	3.70	3.47	4.64	4.78
	1+1 Cu		>5.00	4.35	3.56	3.30	3.92
	1.5+1.5 Cu		>5.00	4.22	3.50	3.14	>5.00
	SMP 101		4.25	4.25	2.45	2.43	3.40
	SMP 301		4.00	3.17	4.00	2.83	4.22
D 2	1 + 1 Cu	48	4.52	4.00	3.50		
D 4			4.68	3.90	4.38		

13. FILM UNSHARPNESS

During some of the image quality investigations the IQI's were also exposed directly on the cassette of the X-ray film, without any filtration of steel. Thus the inherent film unsharpness could be determined by reading the diameter of the smallest wire of the IQI, which was visible in the radiograph.

From fig. 49 the geometric unsharpness can be determined taking into account that:

ϕ = 2o mm (focus size)

F = 2ooo mm (focus-film-distance)

d = o.25 mm (diameter of the thinnest wire)

c = 1.5 mm (thickness of the front side of the cassette)

s = 1.5 mm (largest thickness of the front intensifying screen)

$$U_g = \frac{\phi(s+c+d/2)}{F - (s+c+d/2)} = o.3125 \text{ mm}$$

This geometric unsharpness can be neglected because it is only 12.5% of the diameter of the thinnest wire in the penetrameter (No. 12 - o.25 mm). Therefore the minimum visible wire of the indicator will be the direct measure of film unsharpness.

Table 12 gives the results of film unsharpness measurements, which were made with three sets of ISO IQI's 1/7; 6/12 and 1o/16.

Table 12. Film unsharpness

Film	Screens	Density	Minimum visible wire	
			No.	diameter - mm
GAF 100	1+1 Pb	2.08	11	0.32
GAF 200				
GAF 400				
D 2		2.25	11	0.32
D 4		3.24	10	0.40
M		2.58	11	0.32

Table 12 continued

Film	Screens	Density	Minimum visible wire	
			No.	diameter - mm
GAF 100	1+1 Pb	1.56	10	0.40
GAF 200				
GAF 400		1.44	9	0.50
D 2		1.27	10	0.40
D 4		2.94	11	0.32
M		1.22	10	0.40
GAF 100	1.5+1.5 Pb	1.10	10	0.40
GAF 200		1.30	11	0.32
GAF 400		1.40	10	0.40
D 2		1.65	11	0.32
D 4		2.20	11	0.32
M		1.80	11	0.32
GAF 100	1.5+1.5 Pb	2.20	10	0.40
GAF 200				
GAF 400				
D 2		2.37	11	0.32
D 4		3.39	11	0.32
M		2.42	11	0.32
GAF 100	1.5+1.5 Pb	1.58	9	0.50
GAF 200				
GAF 400		1.42	10	0.40
D 2		1.40	9	0.50
D 4		4.17	10	0.40
M		1.58	11	0.32
GAF 100	1.5+1.5 Pb	1.58	9	0.50
GAF 200		1.30	11	0.32
GAF 400		1.40	10	0.40
D 2		1.65	11	0.32
D 4		2.20	11	0.32
M		1.80	11	0.32
GAF 100	1.5+1.5 Cu	2.98	11	0.32
GAF 200		2.40	12	0.25
GAF 400		1.86	11	0.32
D 2		2.75	12	0.25
D 4		1.68	11	0.32
M		2.46	11	0.32

As can be seen all the films showed an inherent unsharpness better than o.32 mm. This value is quoted by Halmshaw[8] for 2 MeV X-rays, whereas for 1o MeV X-rays o.65 mm can be expected.

14. EXPOSURE CHARTS

From characteristic curves of X-ray films and intensifying screens (see table 1) and the attenuation curve in steel (see fig. 29) exposure charts were computed. Figs. 5o and 51 show the exposure charts for the o.15 + o.25 mm Pb-screens, and fig. 52 gives a comparison for Kodak Microtex and Structurix D2 and D4 films for density 3. On figs. 53 to 55 exposure charts for 1 + 1 mm Pb-screens are shown whereas fig. 56 shows a comparison for Kodak Microtex, Structurix D2 and D4 and GAF 1oo, 2oo and 4oo films.

Similar exposure charts for 1.5 + 1.5 mm Pb-screens are shown on figs. 57 to 6o. Figs. 61 to 63 give the exposure charts for the 1 + 1 mm Cu-screens, and figs. 64 to 67 for the 1.5 + 1.5 mm Cu-screens.

In the way described above (characteristic curves taken without steel filtration + attenuation curve in steel) exposure charts for 1 + 1 mm Pb; 1.5 + 1.5 mm Pb; 1.5 + 1.5 mm Cu-screens were computed whereas exposure charts for the o.15 + o.25 mm Pb; 1 + 1 mm Cu, SMP 1o1; SMP 3o1 screens were computed directly from characteristic curves taken directly through different filtration of steel (see figs. 2o and 22 to 28).

A comparison between the two methods of computing exposure charts are made for Kodak Microtex film exposed with 1 + 1 mm Pb-screen and shows good agreement between these two methods. For that purpose figs. 53 and 68 were used (fig. 68 is taken from [9]).

From the exposure charts, one will see that exposure times were very short. For 25o mm of steel and film density of 3 X-ray films used with the faster fluorometalic screens needed an exposure of only 2.5 min., whereas for the slower films (Structurix D2 or GAF 1oo) an exposure of about 15 min. is needed.

15. SUMMARY OF CONCLUSIONS

From the investigations described the following conclusions can be drawn:

1) It has been proved that radiography of steel up to 25o mm with the Riso 1o MeV linear accelerator is feasible with relatively short exposure times.

2) The investigations have shown that a good radiographic image contract can be obtained (o.5%).

3) To reach better radiographic image quality (as judged by the use of image quality indicators) it is essential to have a smaller focus for the production of X-rays. This is possible, but at the cost of extending exposure times. An attempt will be made in the future to foculize the electron beam on the Bremsstrahlung converter to such an extent, that good IQI sensitivity is obtained.

4) From the point of view of radiographic image contrast Kodak Microtex film witn 1 + 1 mm Pb screens gives best results in thicker steel sections (above 15o mm). In the region from 5o to 15o mm Fe fluorometalic screens give even better radiographic contrast and at the same time reduce exposure time.

5) From the point of view of radiographic image quality (as judged by the wire IQI), thick lead screens (1 + 1 or 1.5 + 1.5 mm) with Kodak Microtex film give the best results. Optimum sensitivity is reached at about 15o mm Fe.

6) For the highest radiographic image contrast and quality, thick lead screens present most advantages with a fine grain film like Kodak Microtex. Such screens are comparatively cheap and easy to handle, which is not true of e.g. tantalum screens, as advertised by several investigators.

16. REFERENCES

1. Brynjolfsson, A., Thaarup, G., Determination of Beam Parameters and Measurements of Dose Distribution in Materials Irradiated by Electrons in the Range of 6 MeV to 14 MeV. Risø Report No. 53, 1963.

2. Hansen, Johnny, A 10 MeV Bremsstrahlung Converter. Risø Report M-1261 ISBN 87 550 0064 9, 1971.

3. Sehested, K., in: Manual on Radiation Dosimetry. Edited by Holm, N.W. and Berry, R.J., Marcel Dekker, New York, 1970.

4. Laurence, G.C., Ball, L.W. and Archibald, W.J., National Research Council of Canada Bulletin, 1942.

5. Johns, H.E. and Garret, C.: Sensitivity and Exposure Graphs for Radium Radiography. Non-Destructive Testing. Winter 1949-50, pp. 16-25.

6. Domanus, J. and Osuchowski, B.: A Comparative Method of Investigation for Optimum Conditions in Radiography by Means of a Slotted Wedge (in Polish). The Problem Sessions Series of the Polish Academy of Sciences. XXVI. Wrocław-Warszawa-Kraków, 1965.

7. American Standards Association. ASA. PH2.8-1964. American Standard Method for the Sensitometry of Industrial X-ray Films for Energies up to 3 Million Electron Volts.

8. Halmshaw, R., Industrial Radiology Techniques. Wykeham Publications (London), Ltd., 1971.

9. Domanus, J., Analysis of Exposure Factors Influencing the Image Quality in Linear Accelerator Radiography. Risø-M-1579, 1973.

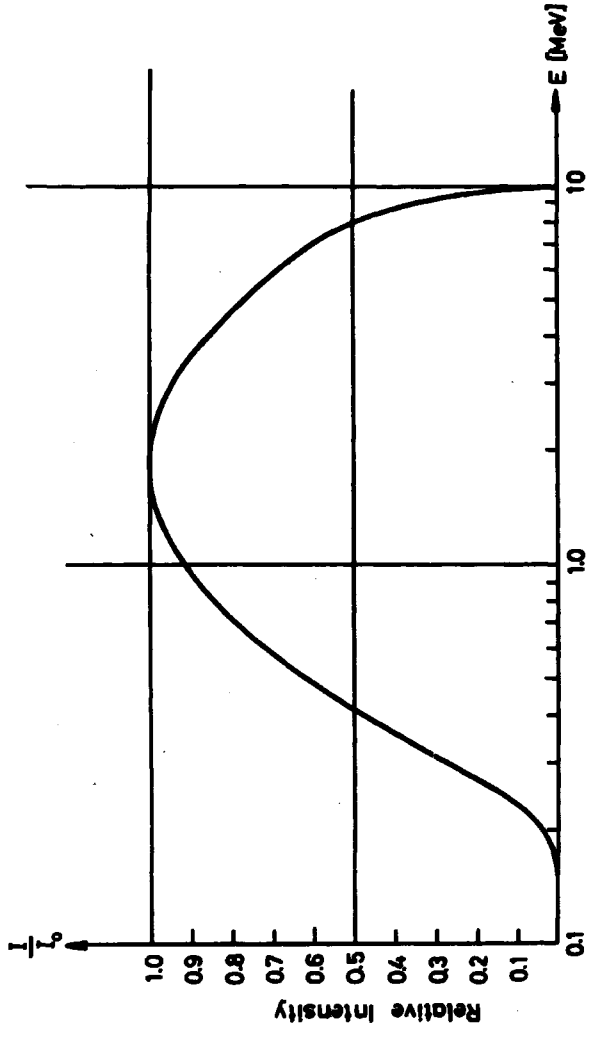

Fig. 1. Calculated 10 MeV Bremsstrahlung spectrum for the converter.

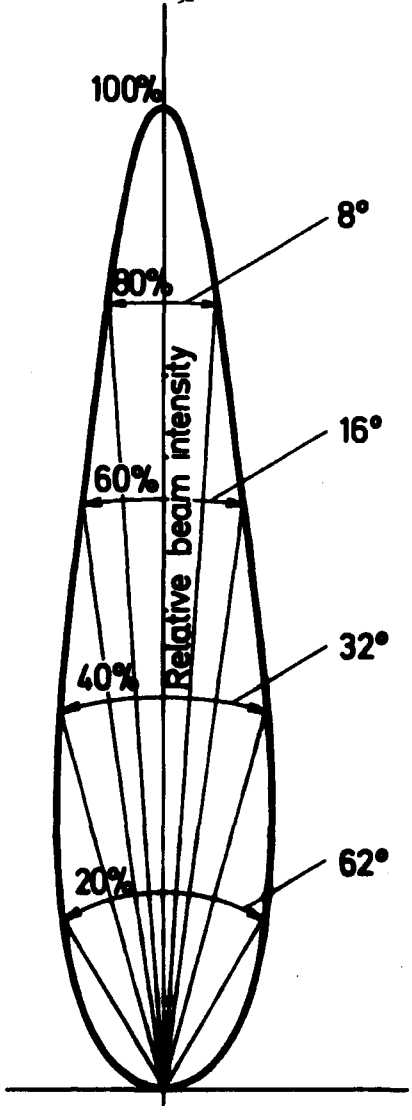

Fig. 2. Intensity distribution in the X-ray beam.

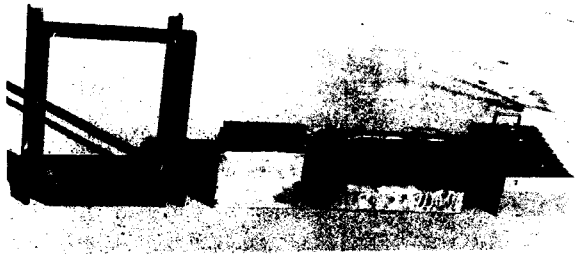

Fig. 3. Elements (50 mm thick) of the steel block.

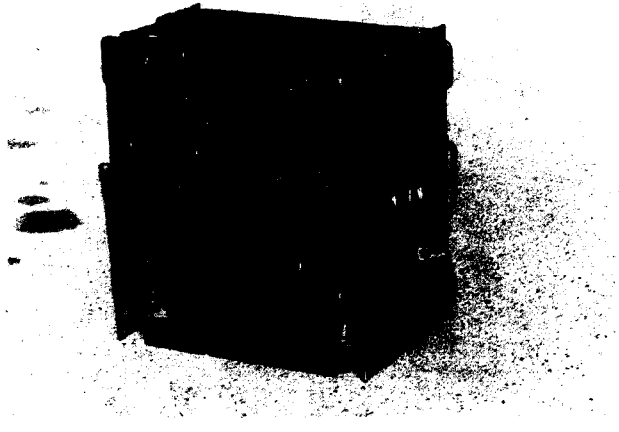

Fig. 4. Steel block after assembly.

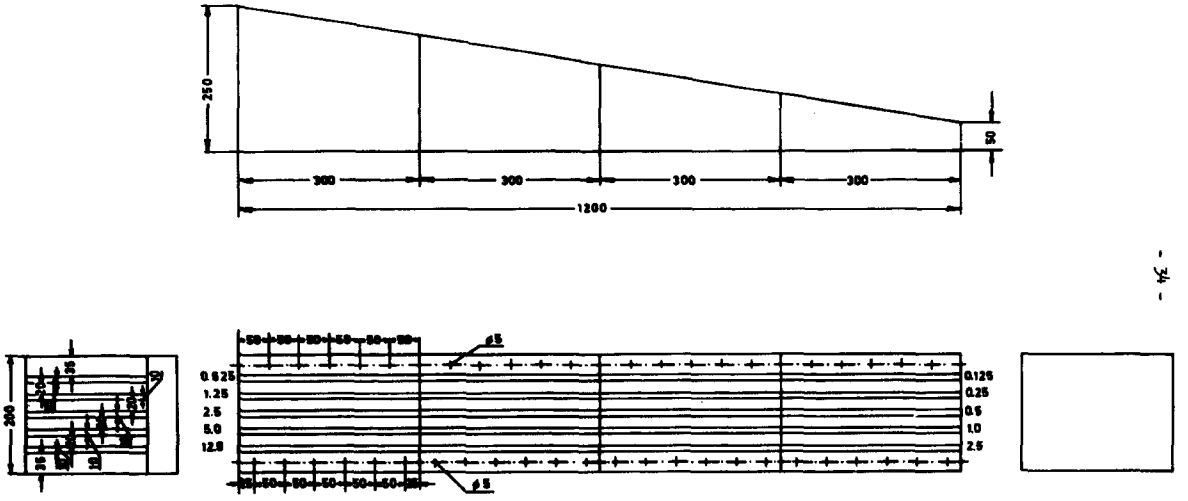

Fig. 5. Construction of the slotted steel wedge.

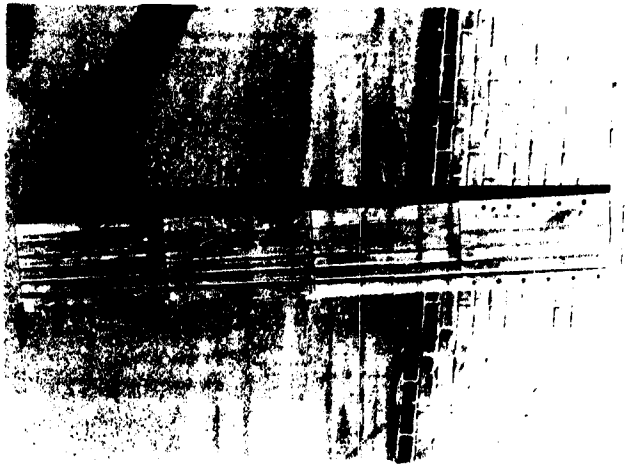

Fig. 6. Steel wedge in its full length.

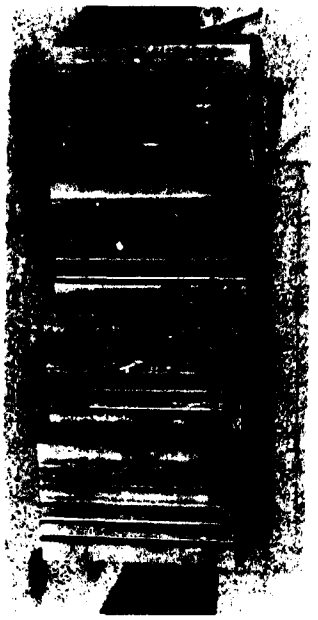

Fig. 7. Four slotted steel wedges.

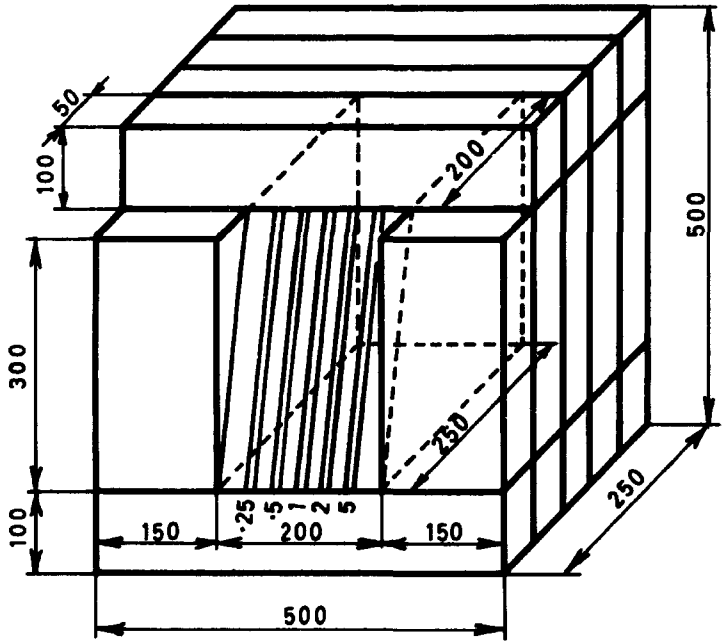

Fig. 8. Slotted steel wedge surrounded with masking plates.

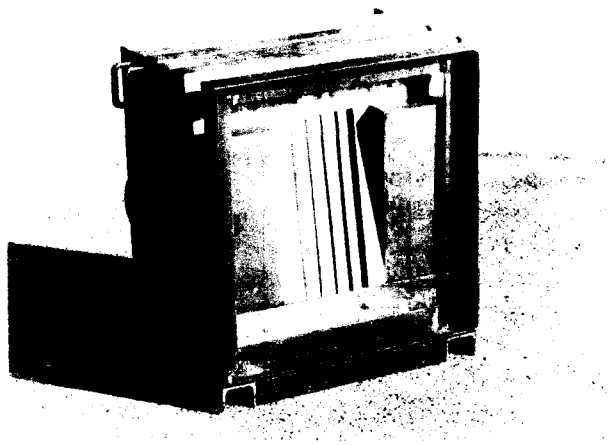

Fig. 9. Assembled steel blok with slotted wedge.

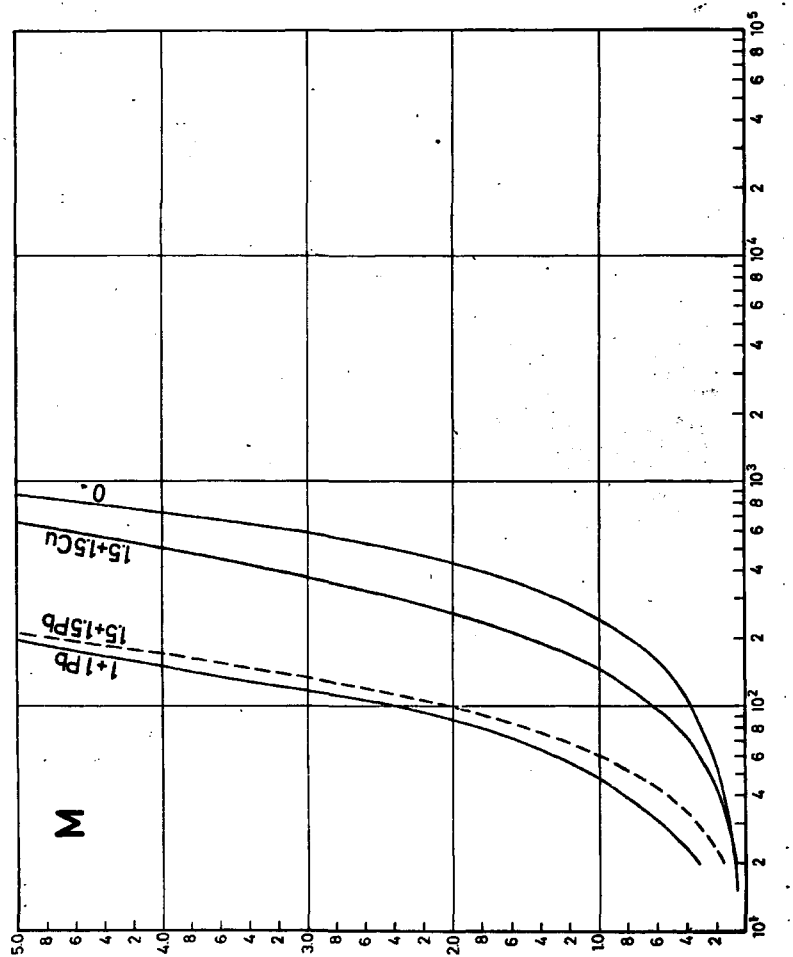

Fig. 10. Characteristic curves (no filtration) for Kodak Microtex films.

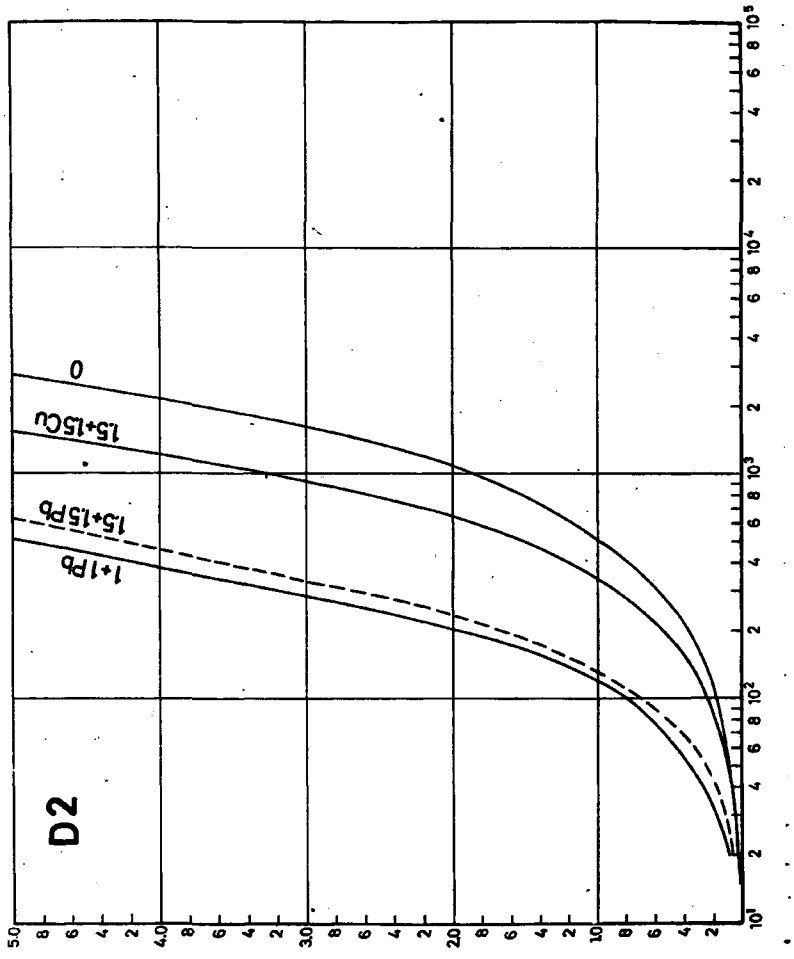

Fig. 11. Characteristic curves (no filtration) for Structurix D 2 films.

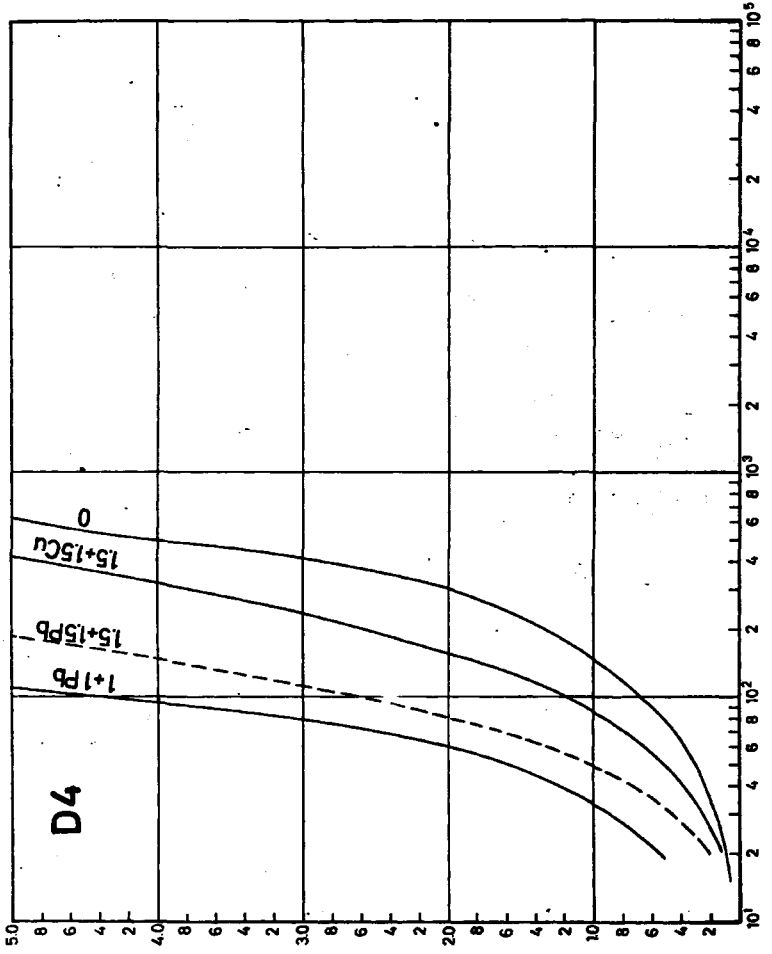

Fig. 12. Characteristic curves (no filtration) for Structurix D 4 films.

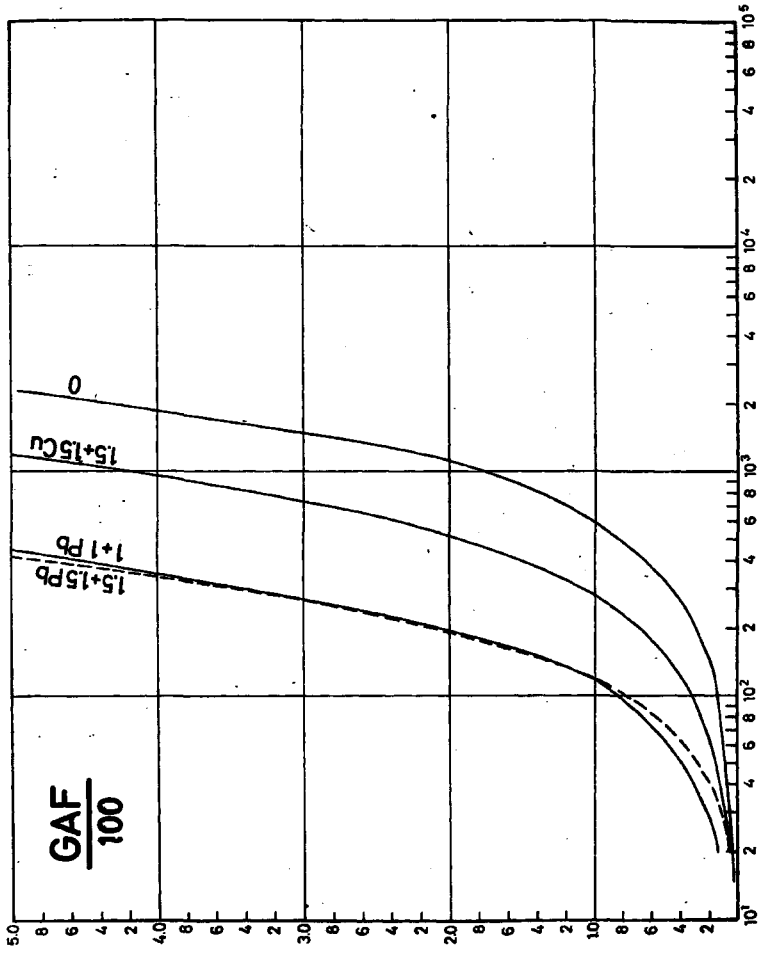

Fig. 13. Characteristic curves (no filtration) for GAF 100 films.

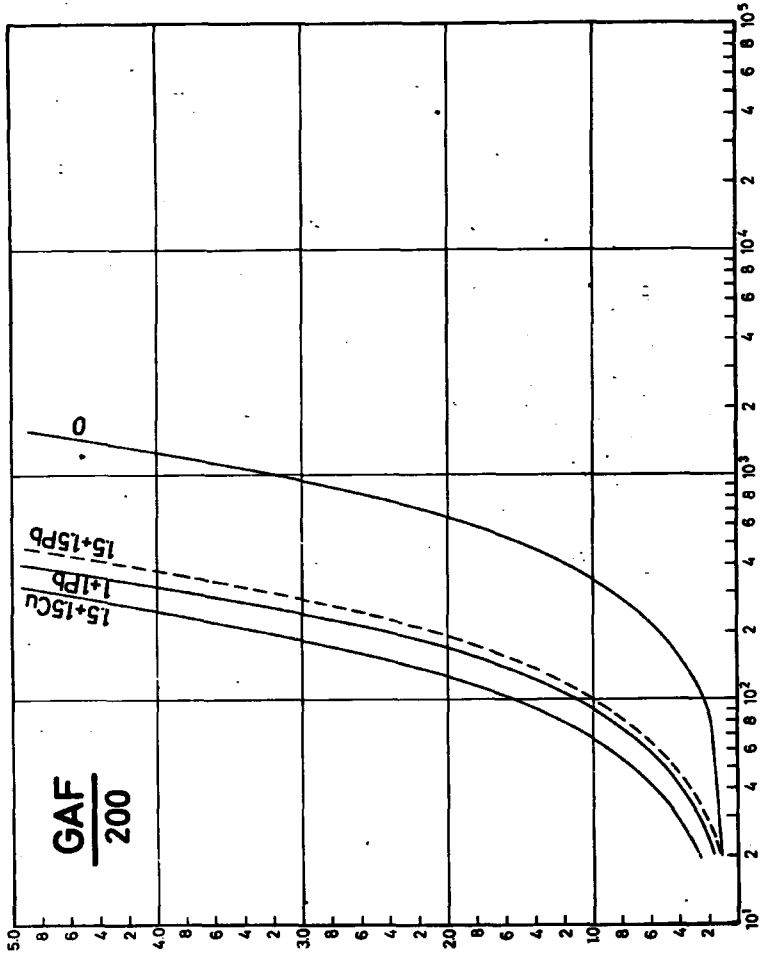

Fig. 14. Characteristic curves (no filtration) for GAF 200 films.

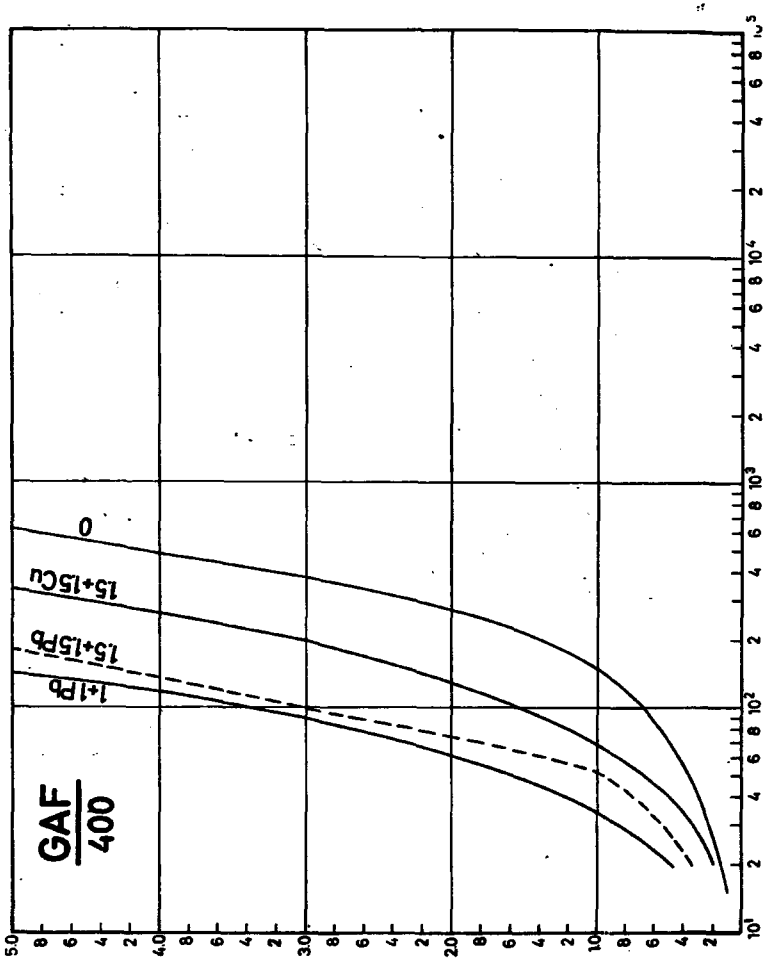

Fig. 15. Characteristic curves (no filtration) for GAF 400 films.

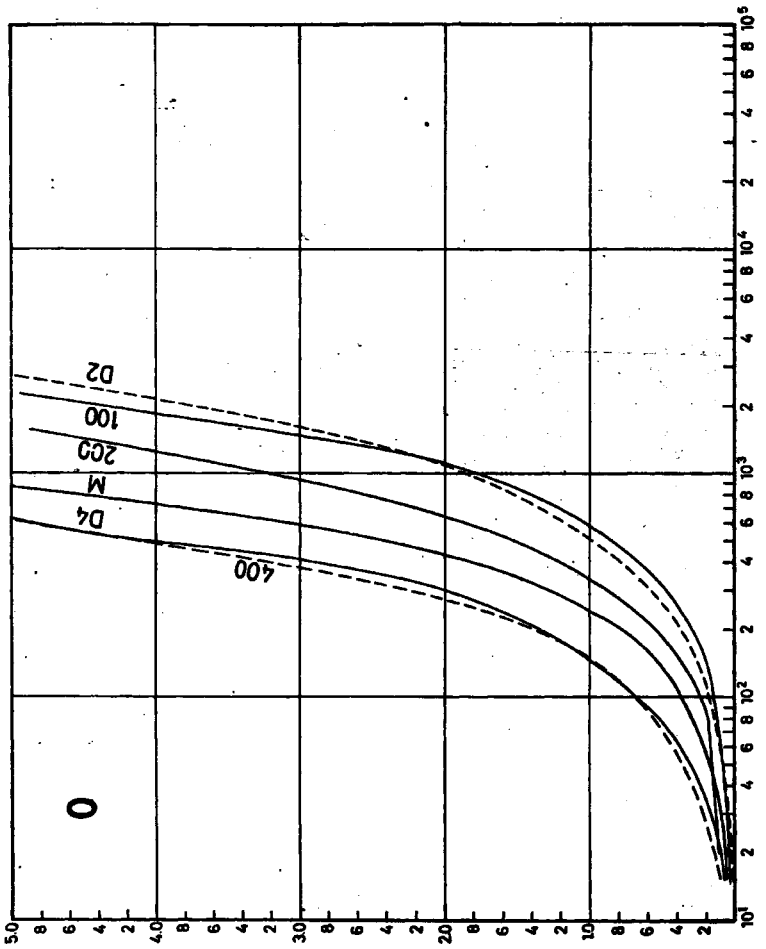

Fig. 16. Characteristic curves (no filtration) without intensifying screens.

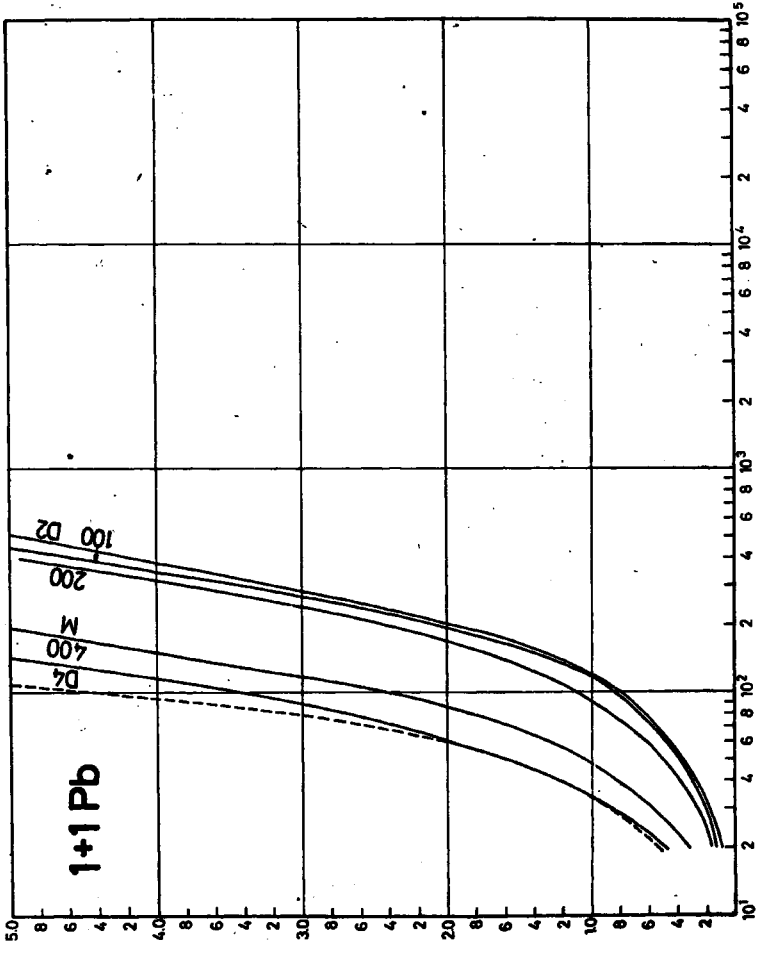

Fig. 17. Characteristic curves (no filtration) with 1+1 mm Pb screens.

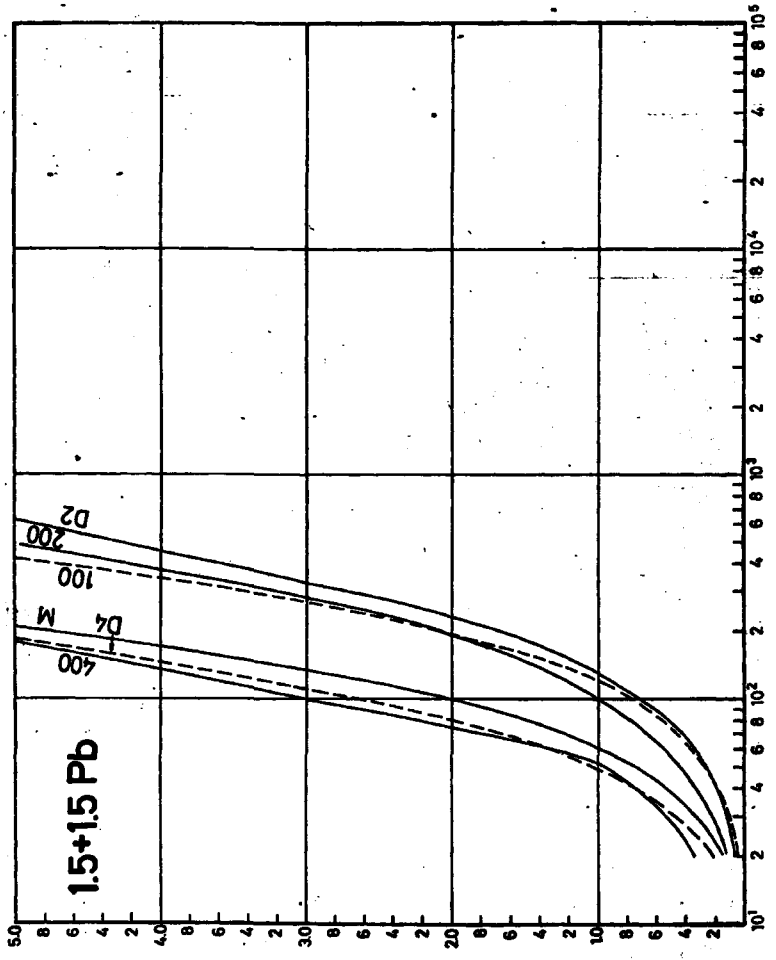

Fig. 18. Characteristic curves (no filtration) with 1.5+1.5 mm Pb screens.

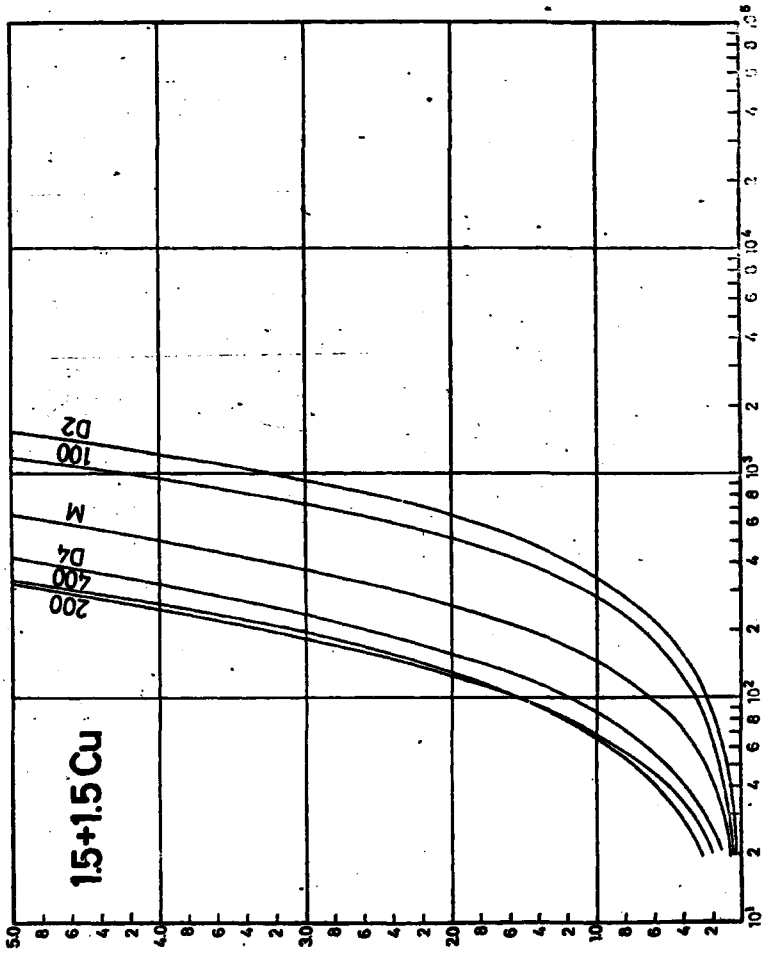

Fig. 19. Characteristic curves (no filtration) with 1.5+1.5 mm Cu screens

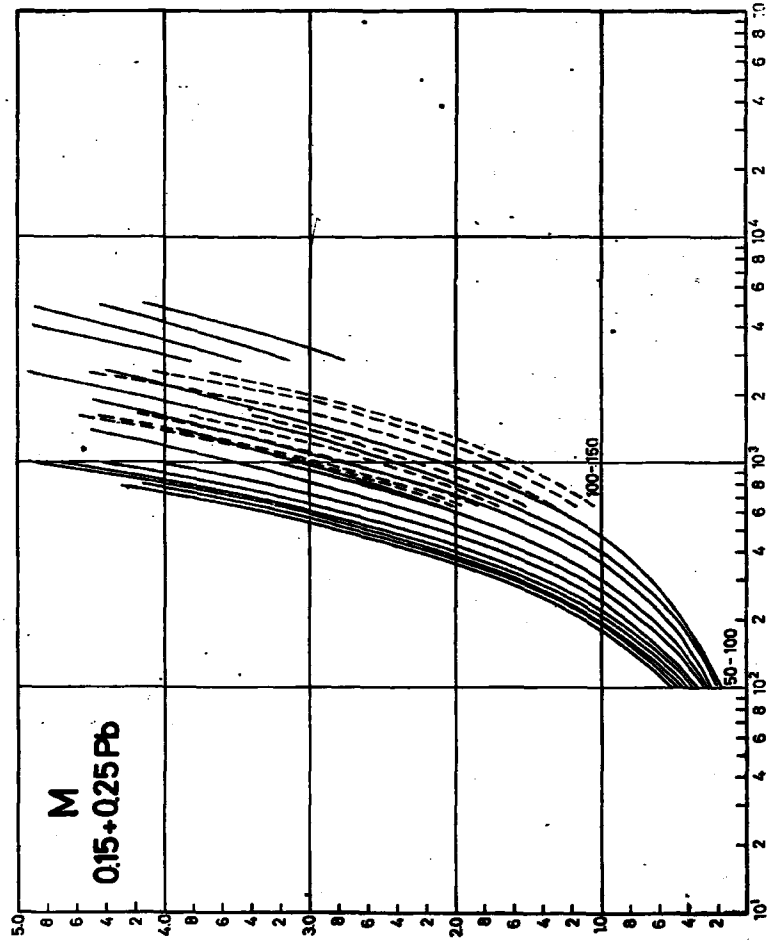

Fig. 20. Characteristic curves (through 50-150 mm Fe) for Kodak Microtex films with 0.15+0.25 Pb screens.

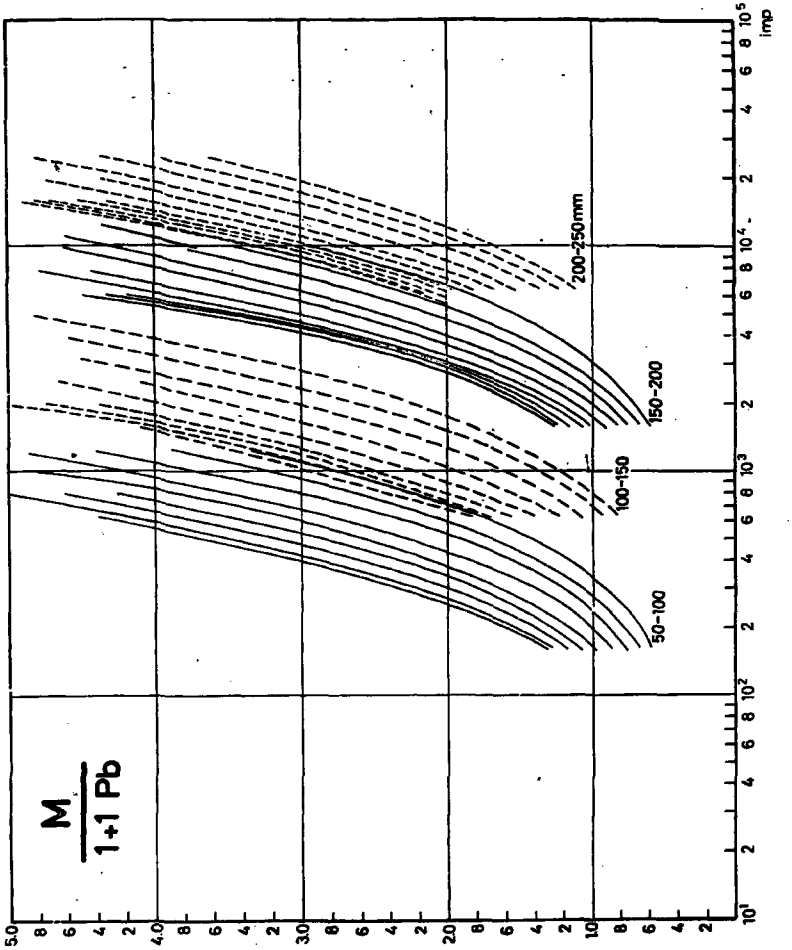

Fig. 21. Characteristic curves (through 50-250 mm Fe) for Kodak Microtex films with 1+1 mm Pb screens.

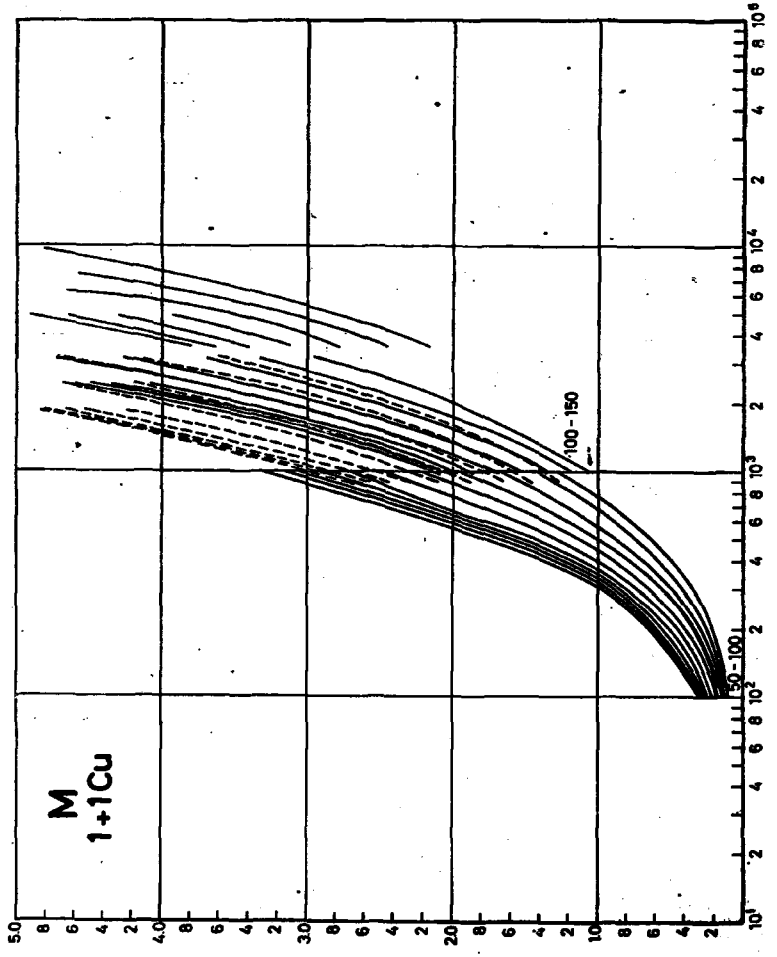

Fig. 22. Characteristic curves (through 50-150 mm Fe) for Kodak Microtex films with 1+1 mm Cu screens.

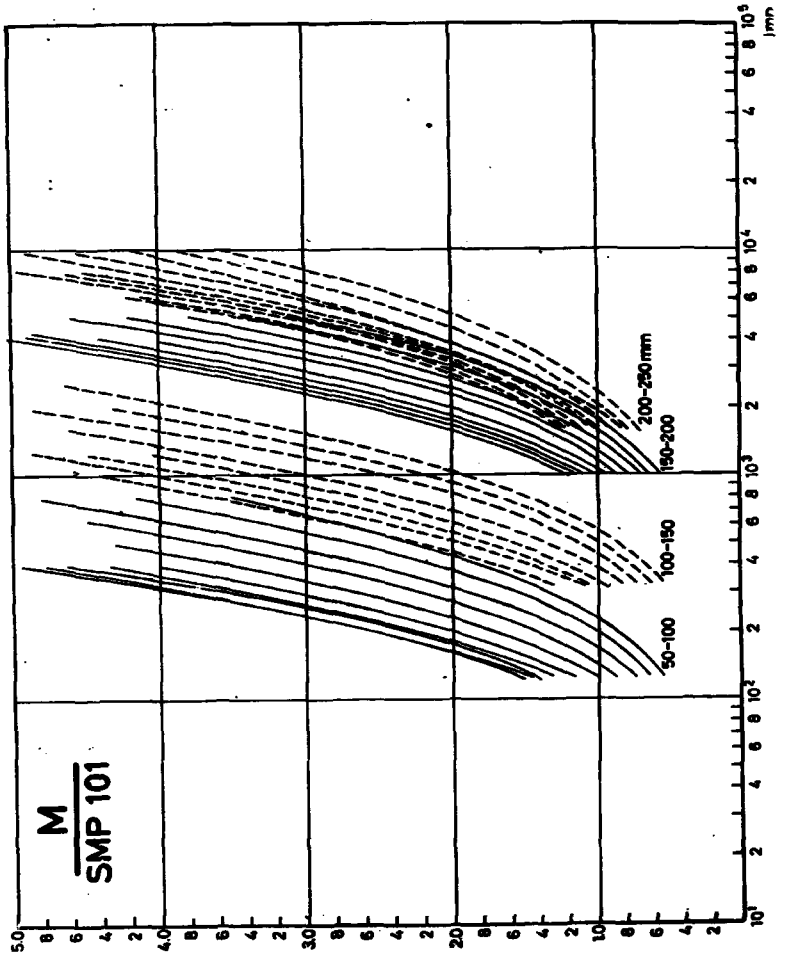

Fig. 23. Characteristic curves (through 50-250 mm Fe) for Kodak Microtex films with SMP 101 screens.

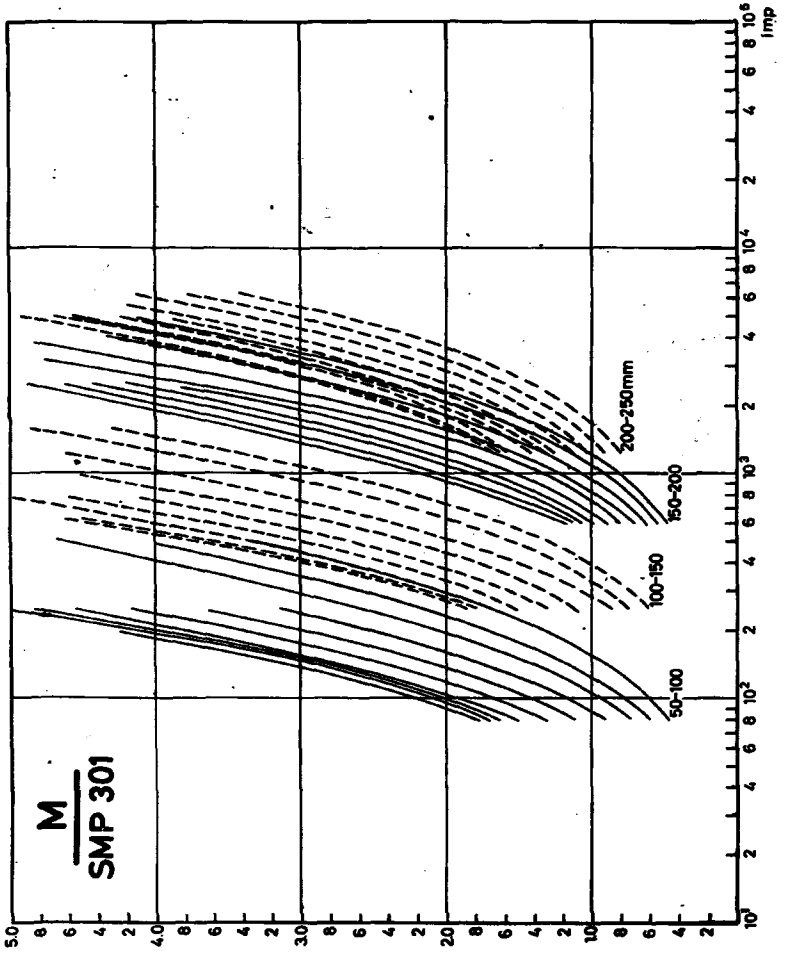

Fig. 24. Characteristic curves (through 50-250 mm Fe) for Kodak Microtex films with SMP 301 screens.

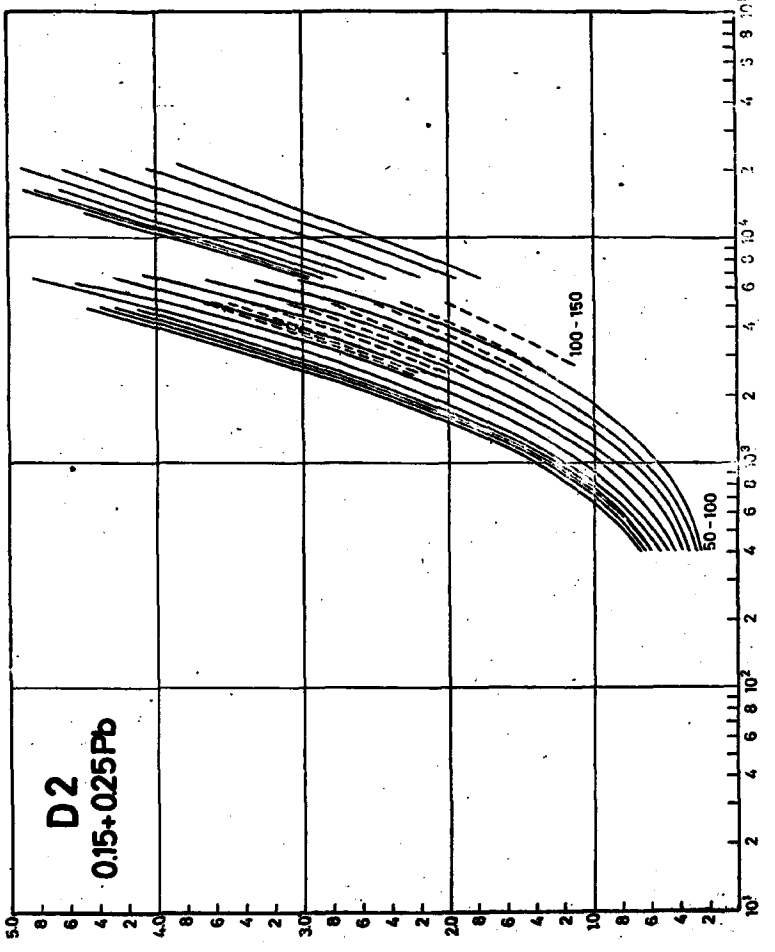

Fig. 25. Characteristic curves (through 50-150 mm Fe) for Structurix D 2 films with 0.15+0.25 mm Pb screens.

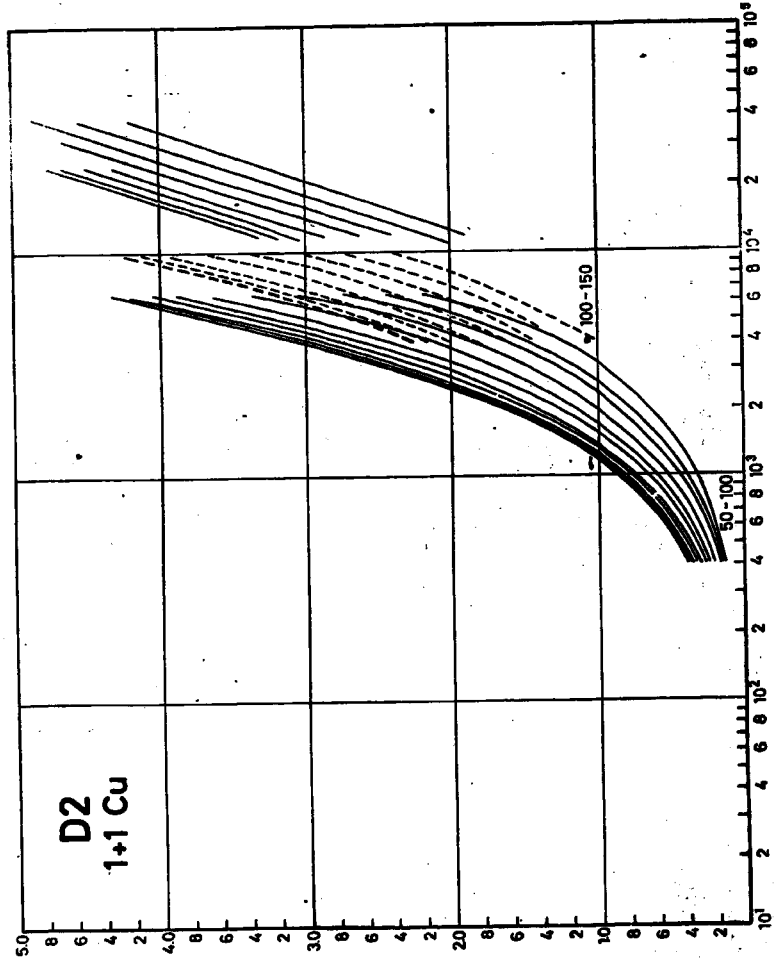

Fig. 26. Characteristic curves (through 50-150 mm Fe) for Structurix D 2 films with 1+1 mm Cu screens.

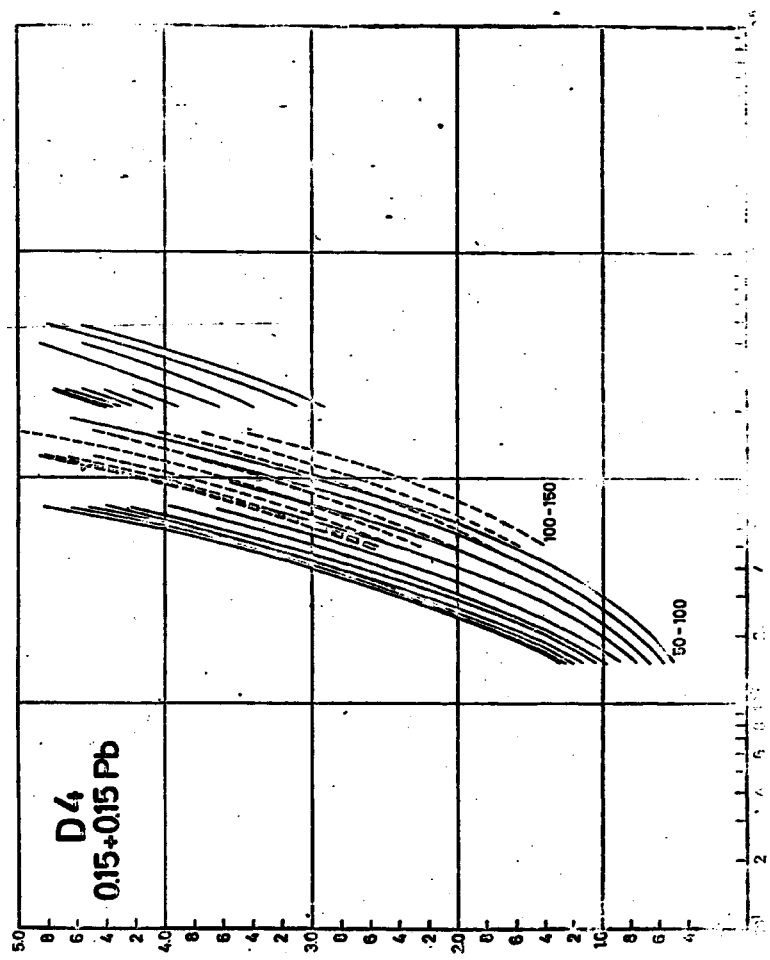

Fig. 27. Characteristic curves (through 50-150 mm Fe) for Structurix D 4 films with 0.15+0.25 mm Pb screens.

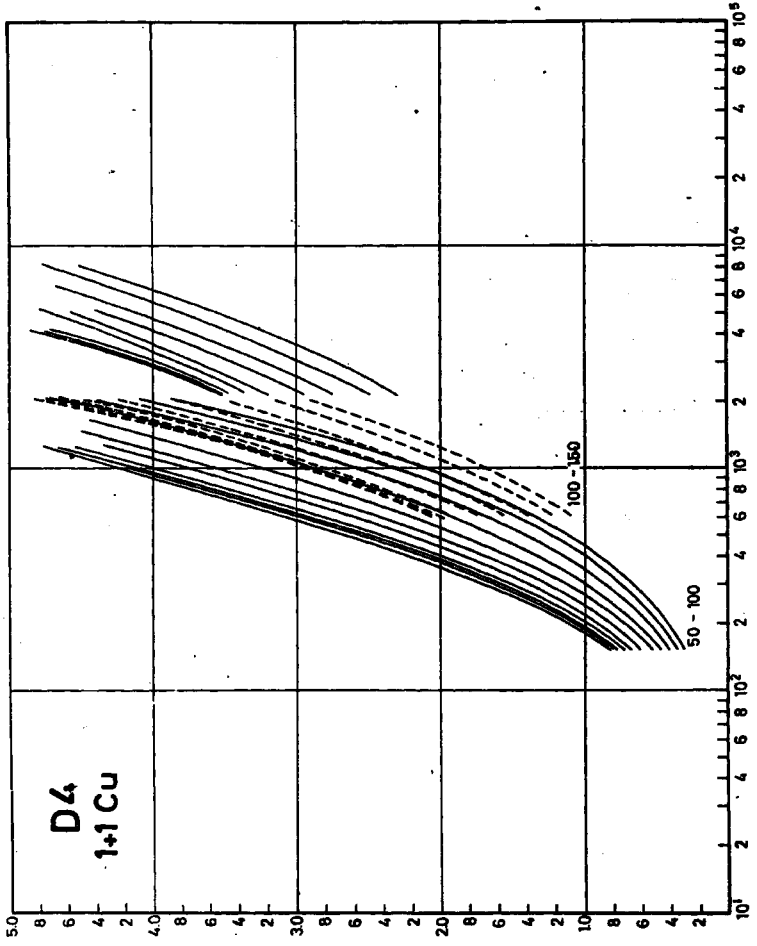

Fig. 28. Characteristic curves (through 50-150 mm Fe) for Structurix D 4 films with 1+1 Cu screens.

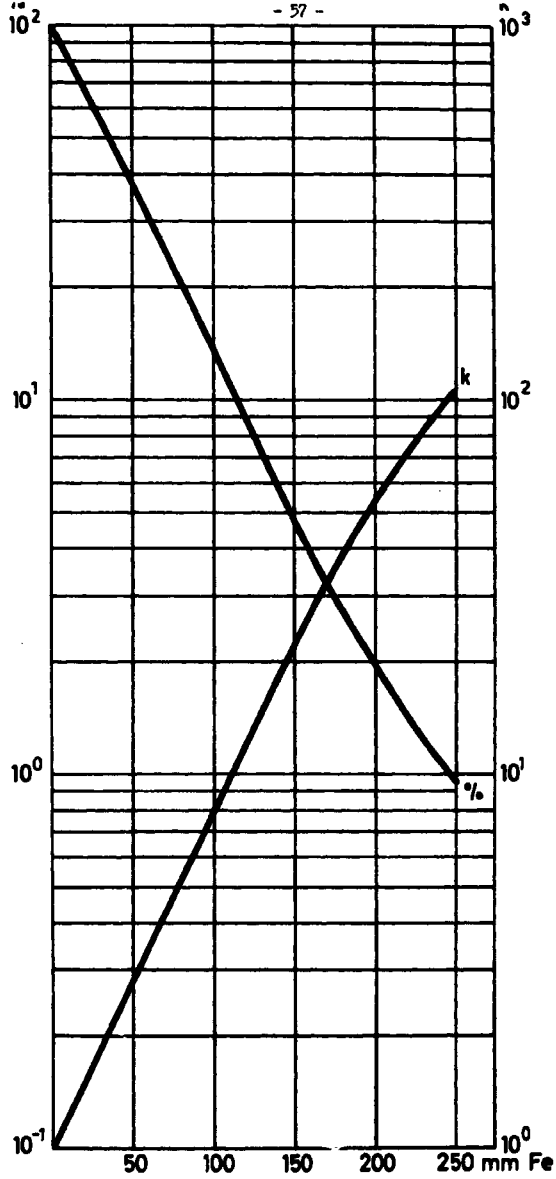

Fig. 29. Attenuation curve in steel.

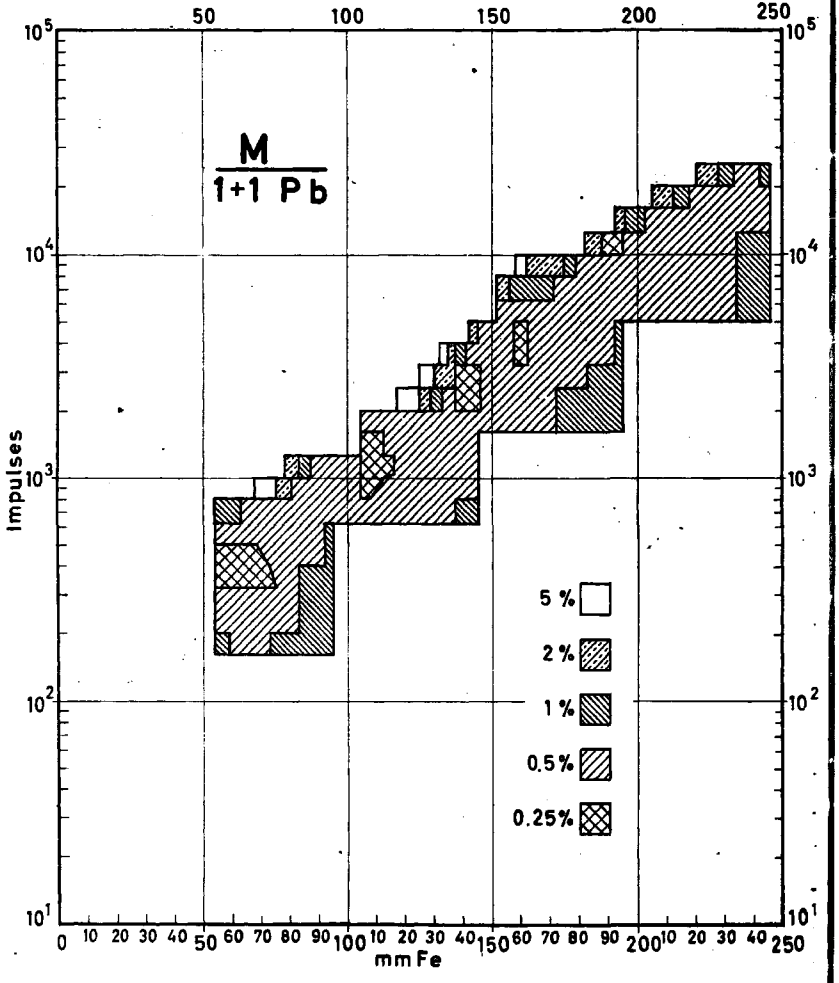

Fig. 30. Visibility of slotted wedge on Kodak M film with 1+1 mm Pb screens.

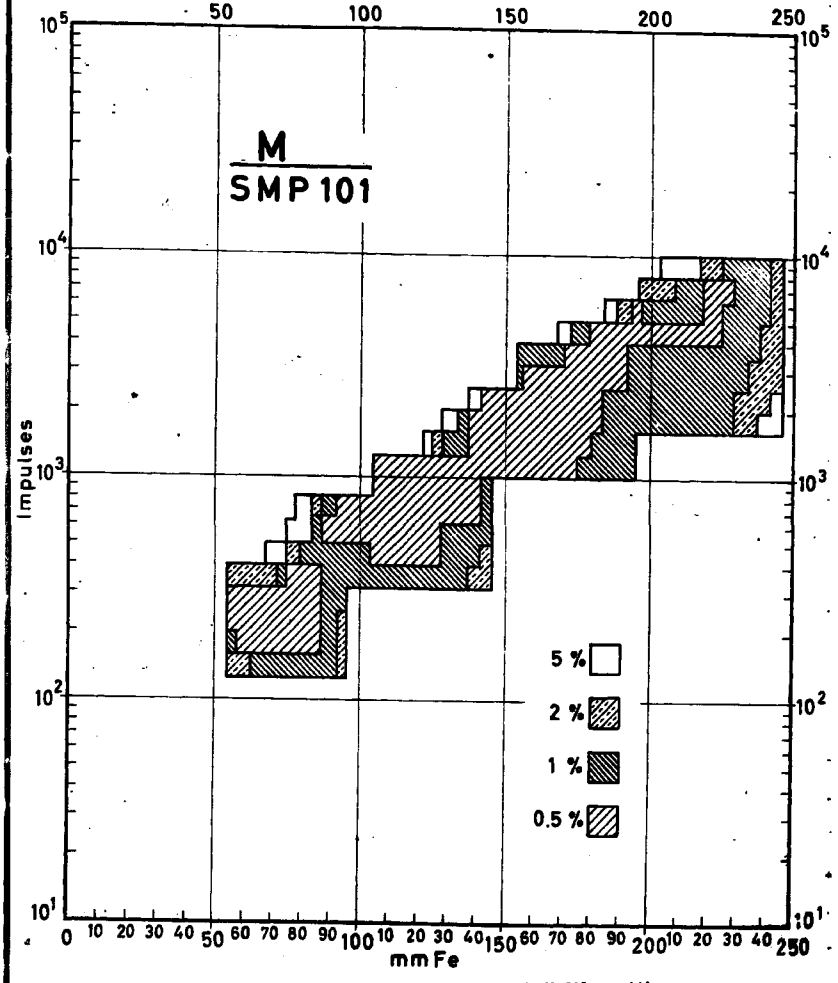

Fig. 31. Visibility of slotted wedge on Kodak M films with SMP 101 screens.

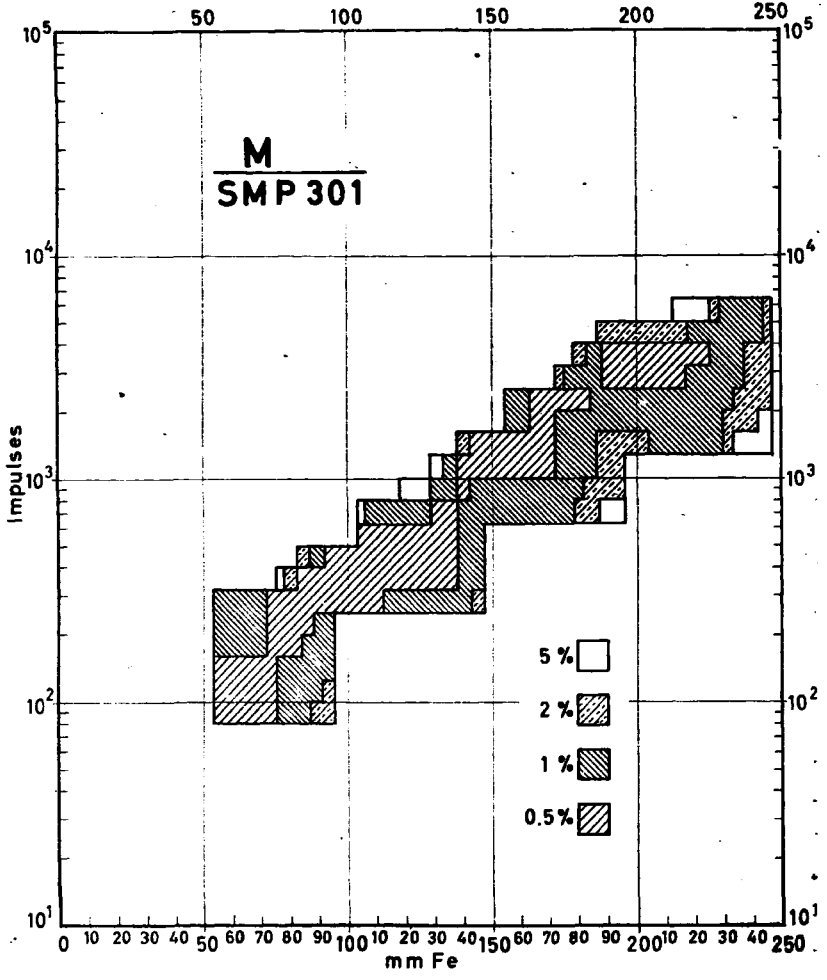

Fig. 32. Visibility of slotted wedge on Kodak M films with SMP 301 screens.

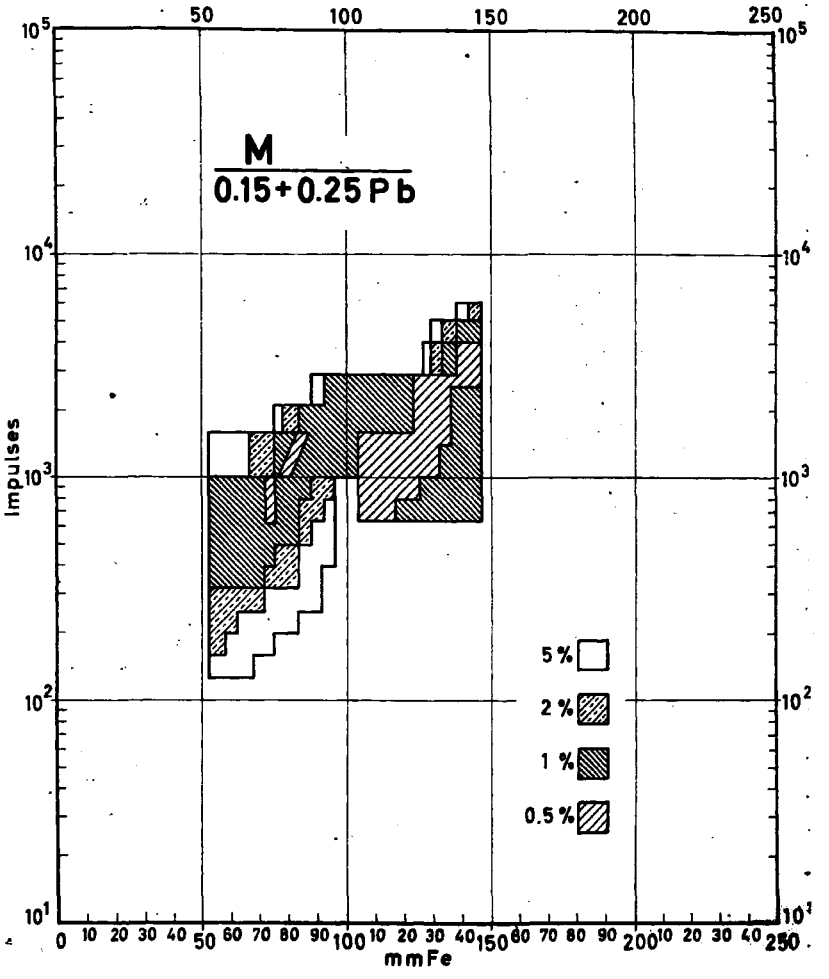

Fig. 33. Visibility of slotted wedge on Kodak M films with 0.15+0.25 mm Pb screens.

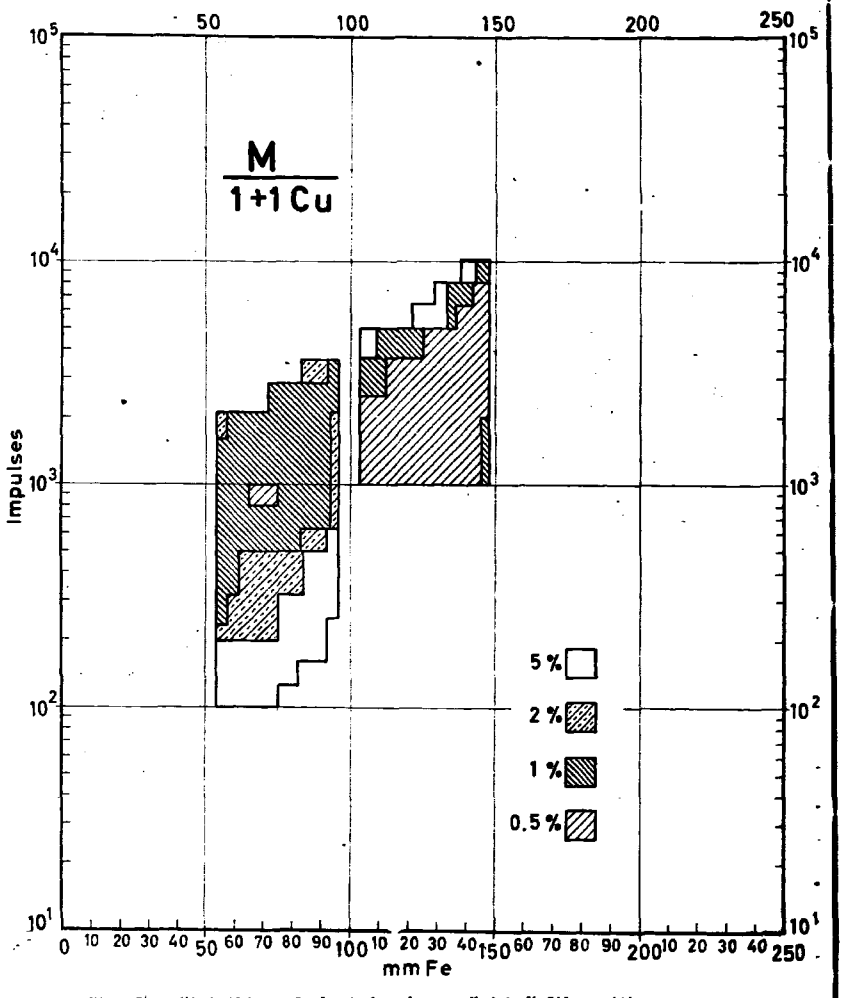

Fig. 34. Visibility of slotted wedge on Kodak M films with 1+1 mm Cu screens.

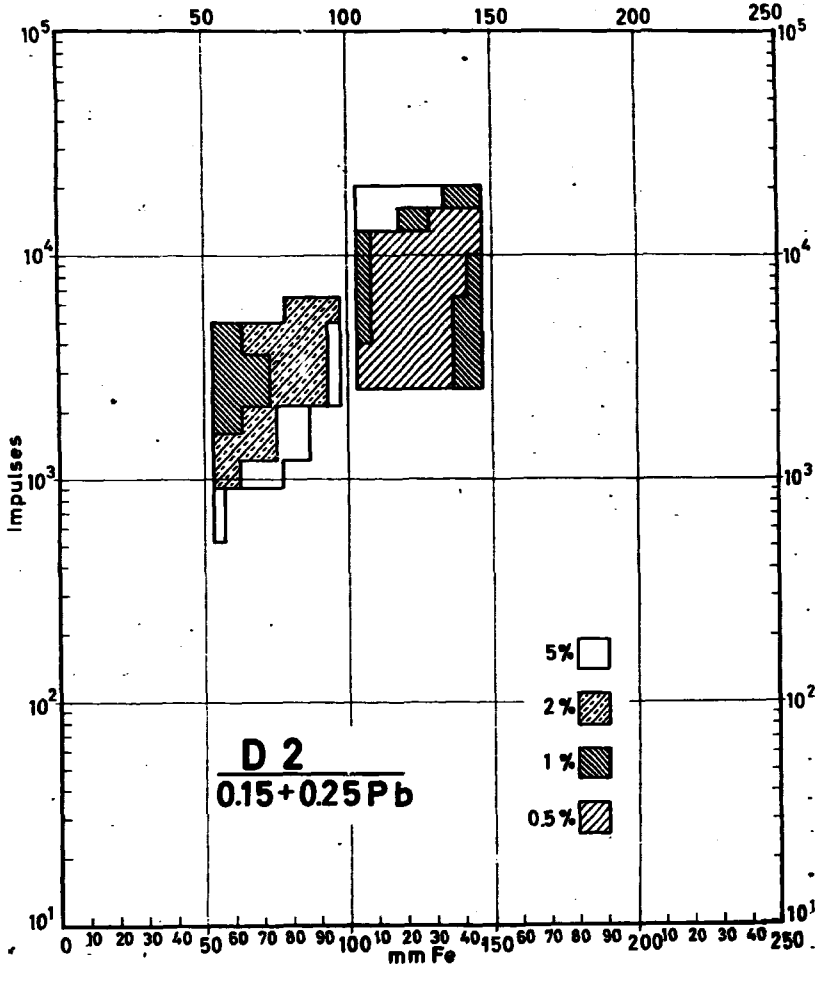

Fig. 35. Visibility of slotted wedge on Structurix D 2 films with 0.15+0.25 mm Pb screens.

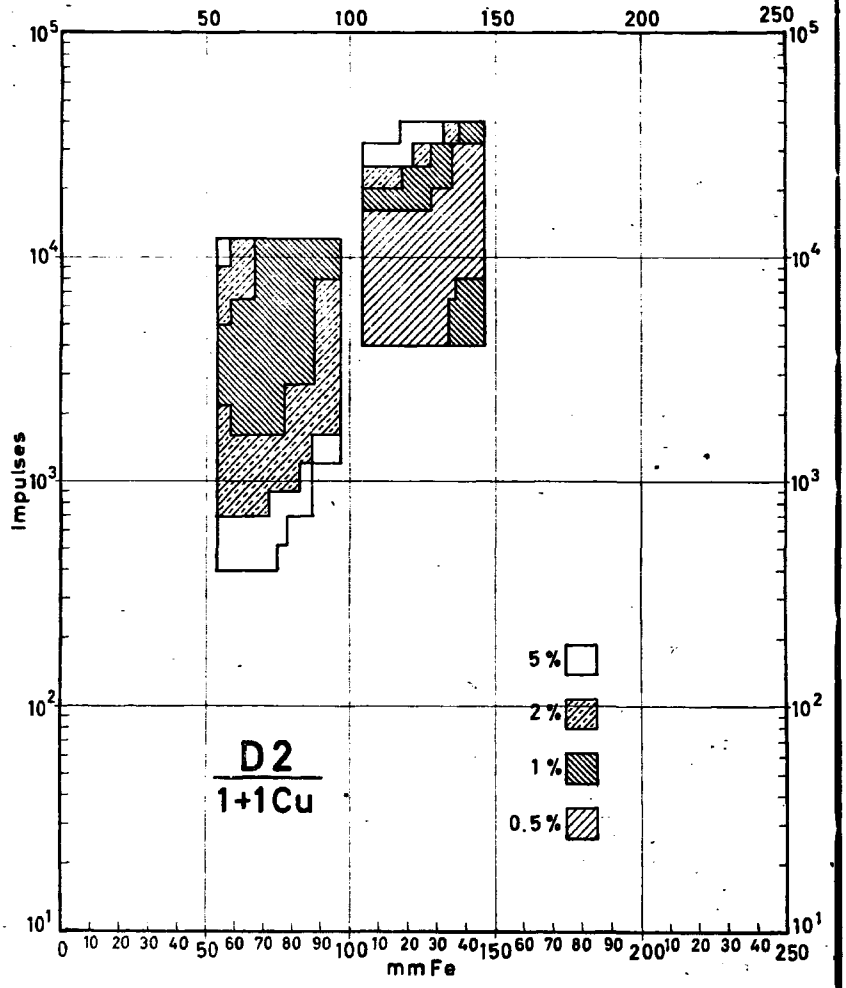

Fig. 36. Visibility of slotted wedge on Structurix D 2 films with 1+1 mm Cu screens.

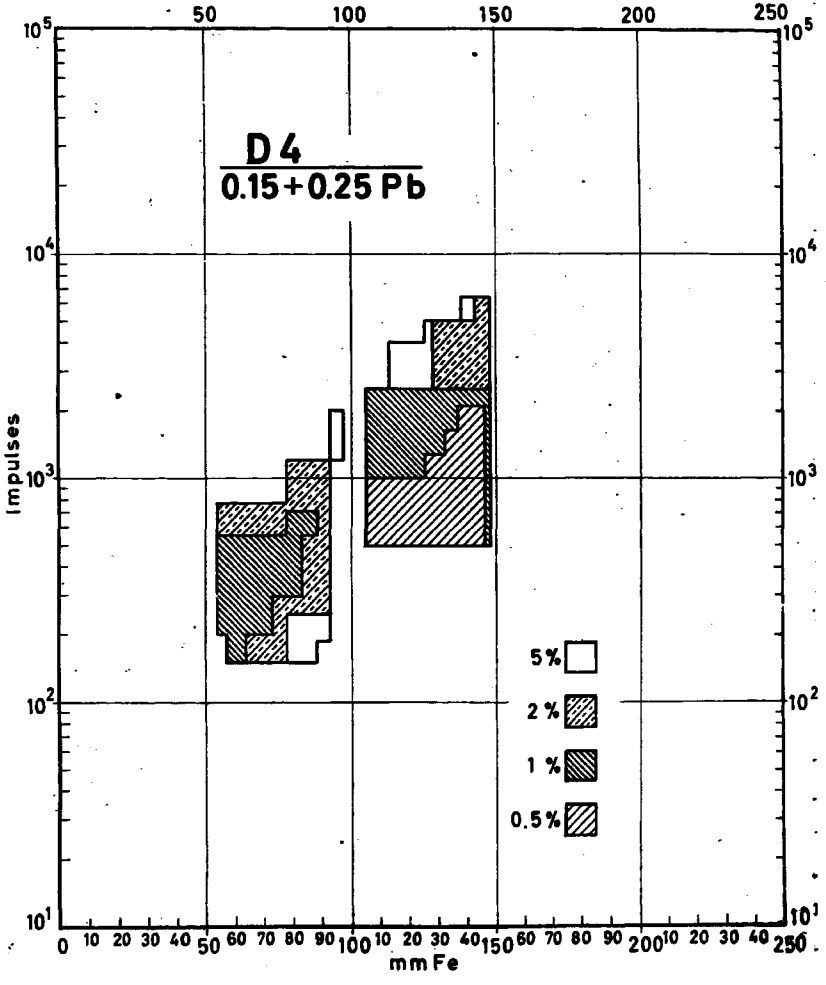

Fig. 37. Visibility of slotted wedge on Structurix D 4 films with 0.15+0.25 mm Pb screens.

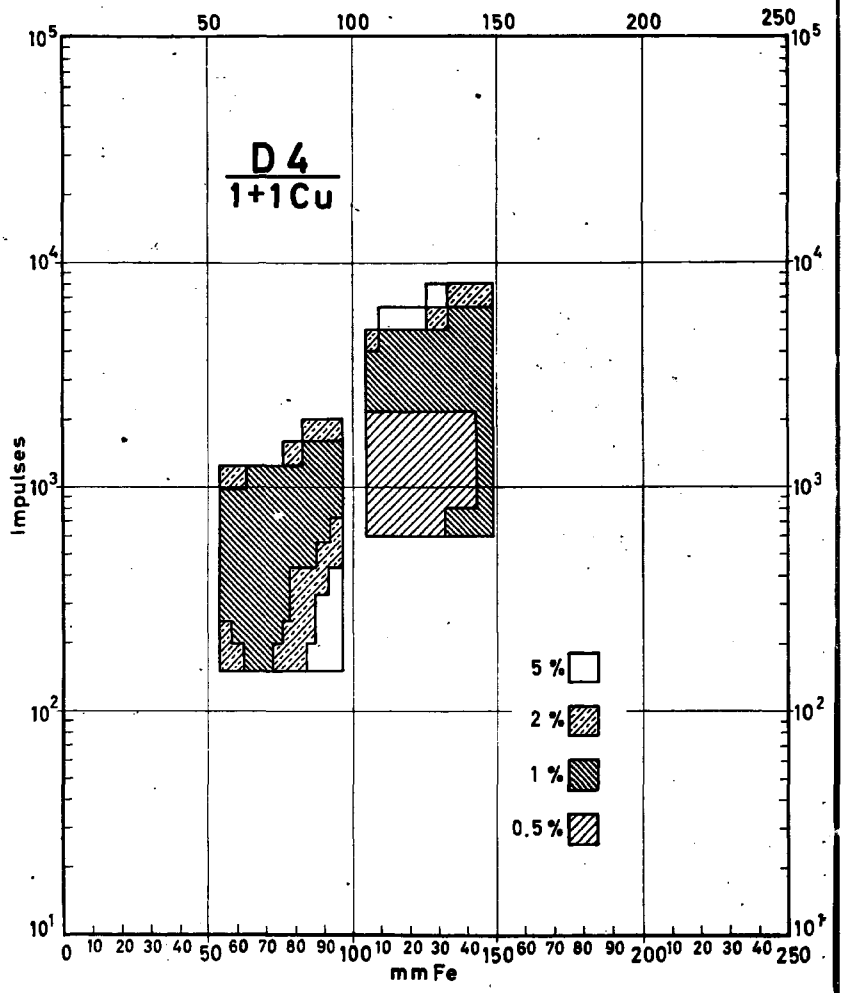

Fig. 38. Visibility of slotted wedge on Structurix D 4 films with 1+1 mm Cu screens.

Fig. 39. Scanning densitometer.

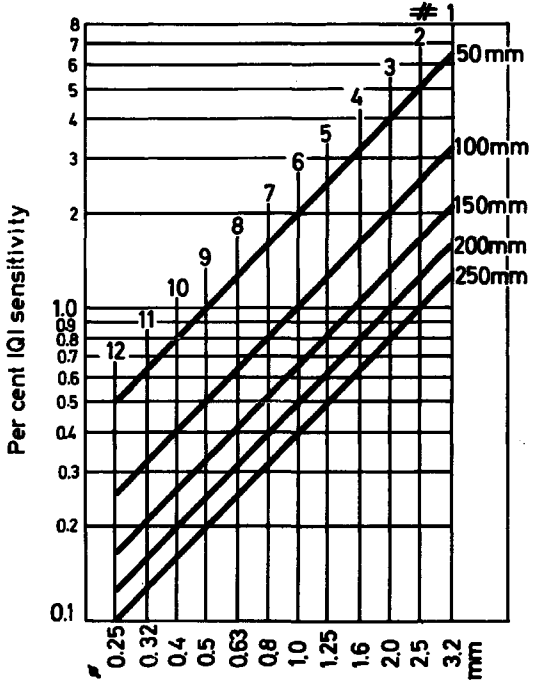

Fig. 40. Per cent IQI sensitivity.

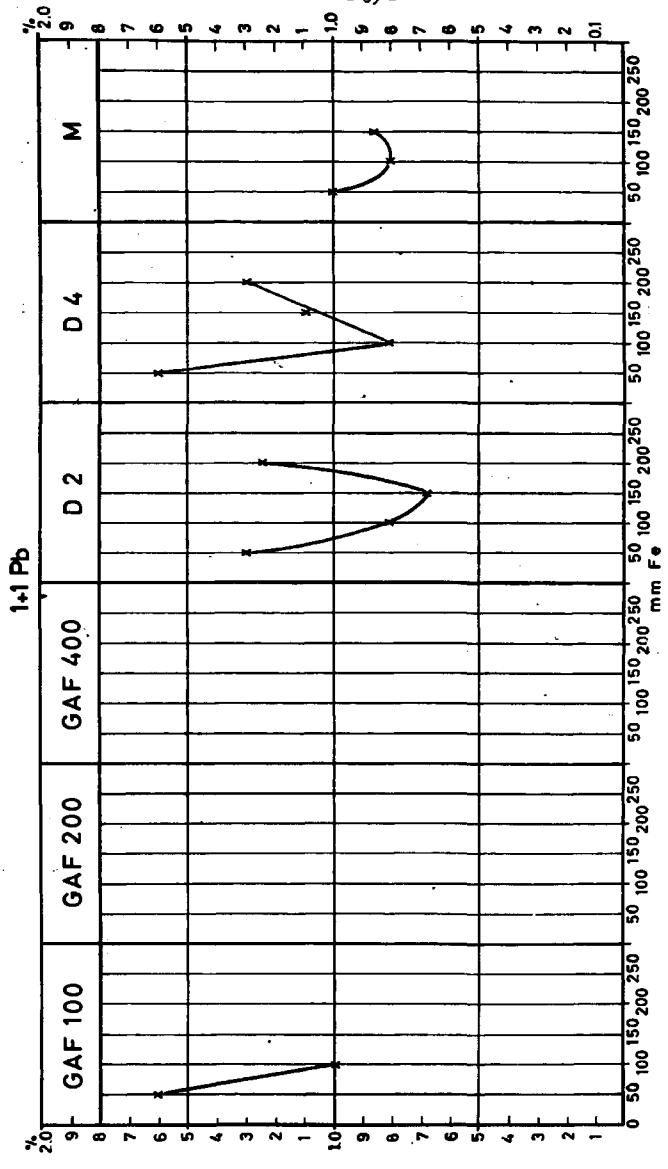

Fig. 41. IQI sensitivities for 1+1 mm Pb screens.

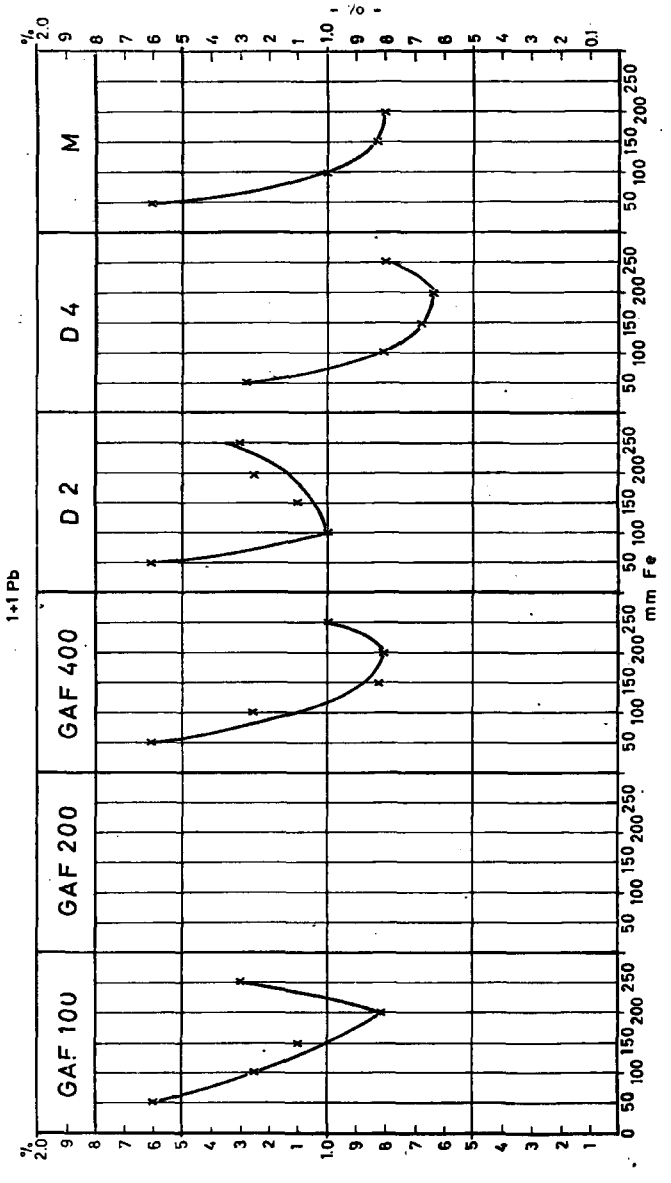

Fig. 42. IQI sensitivities for 1+1 mm Pb screens.

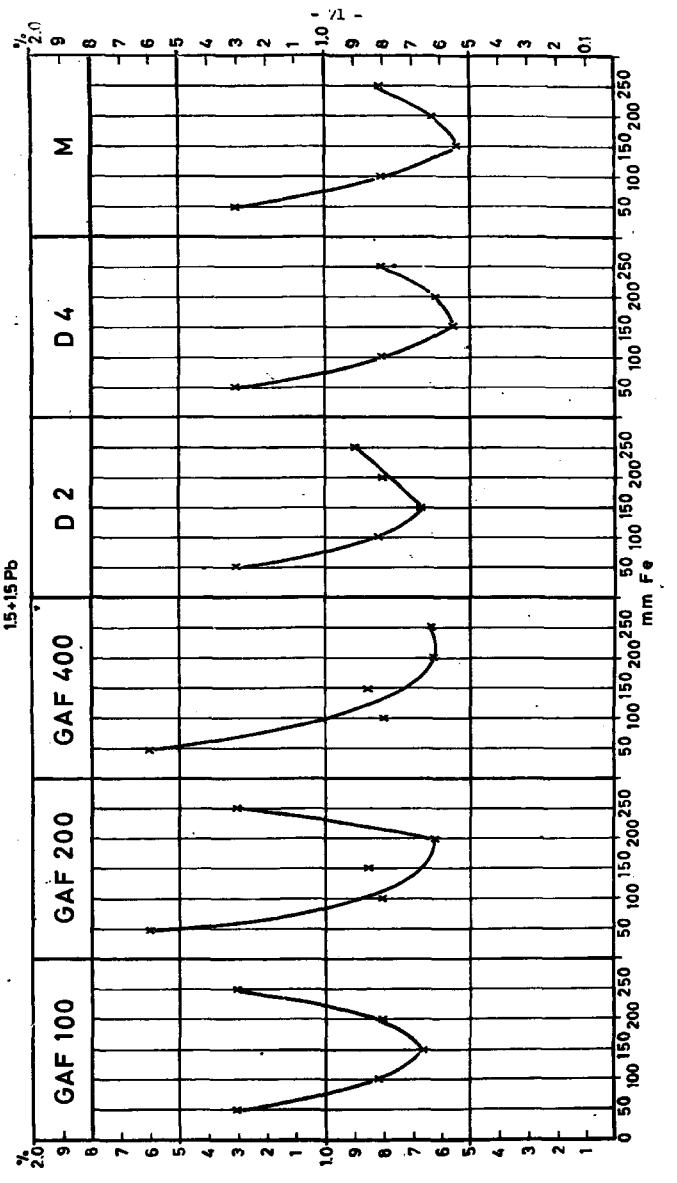

Fig. 43. IQI sensitivities for 1.5+1.5 mm Pb screens.

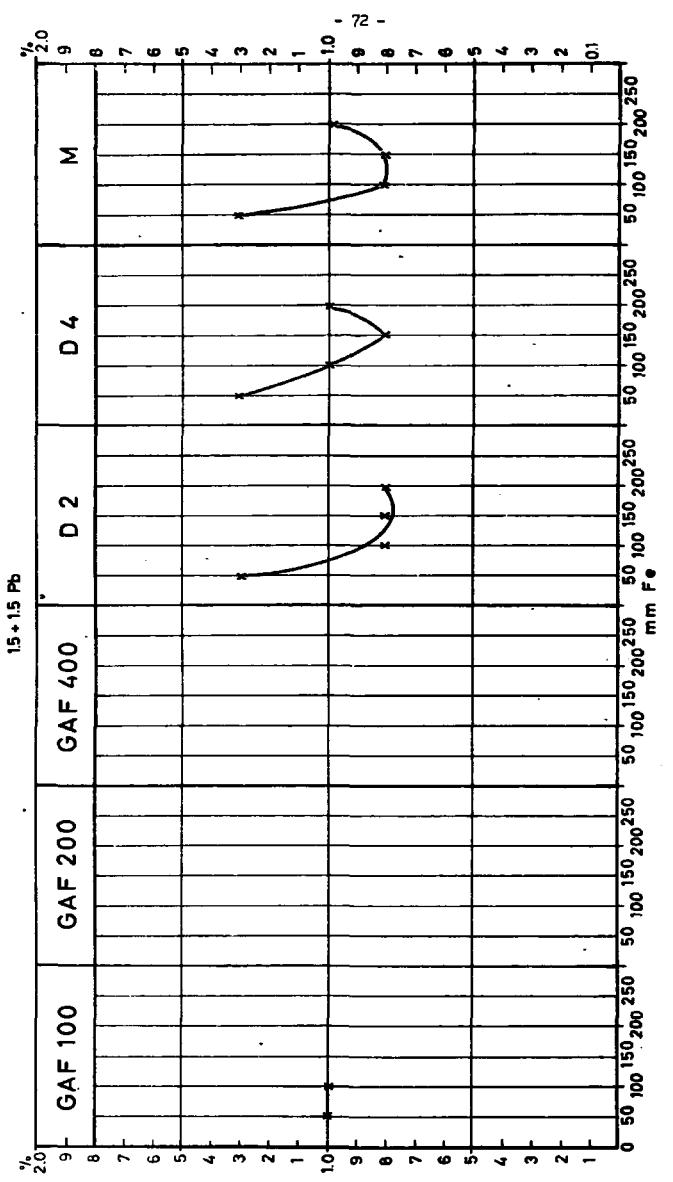

Fig. 44. IQI sensitivities for 1.5+1.5 mm Pb screens.

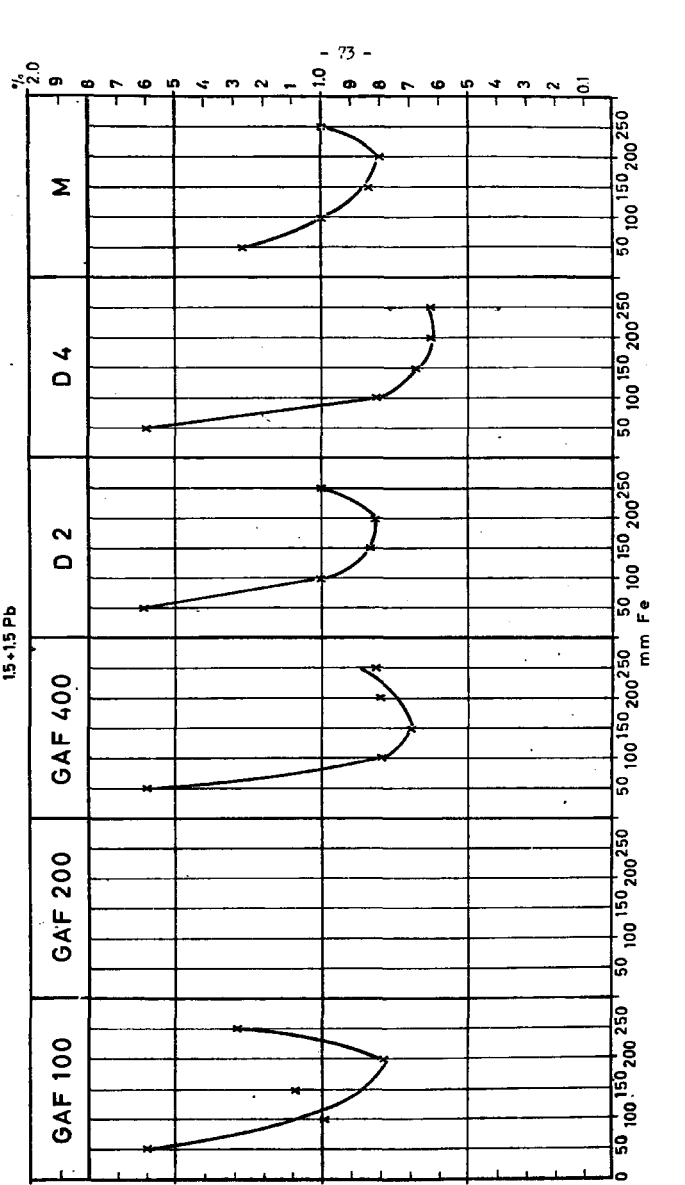

Fig.45. IQI sensitivities for 1.5 + 1.5 mm Pb screens

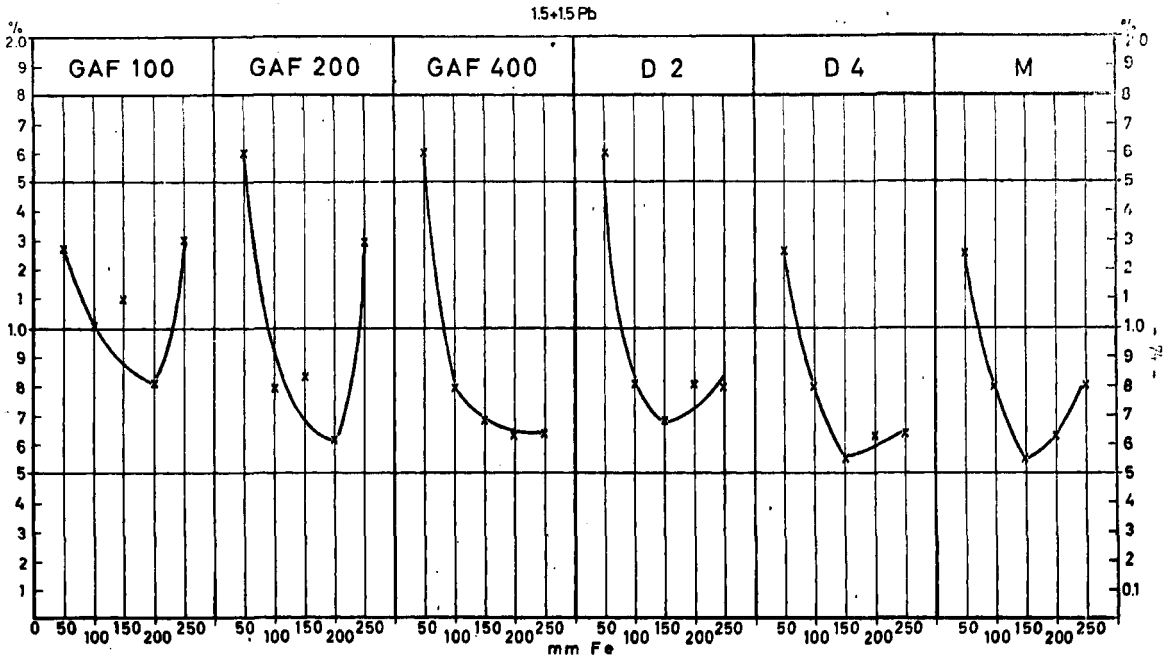

Fig.46. IQI sensitivities for 1.5 + 1.5 mm Pb screens

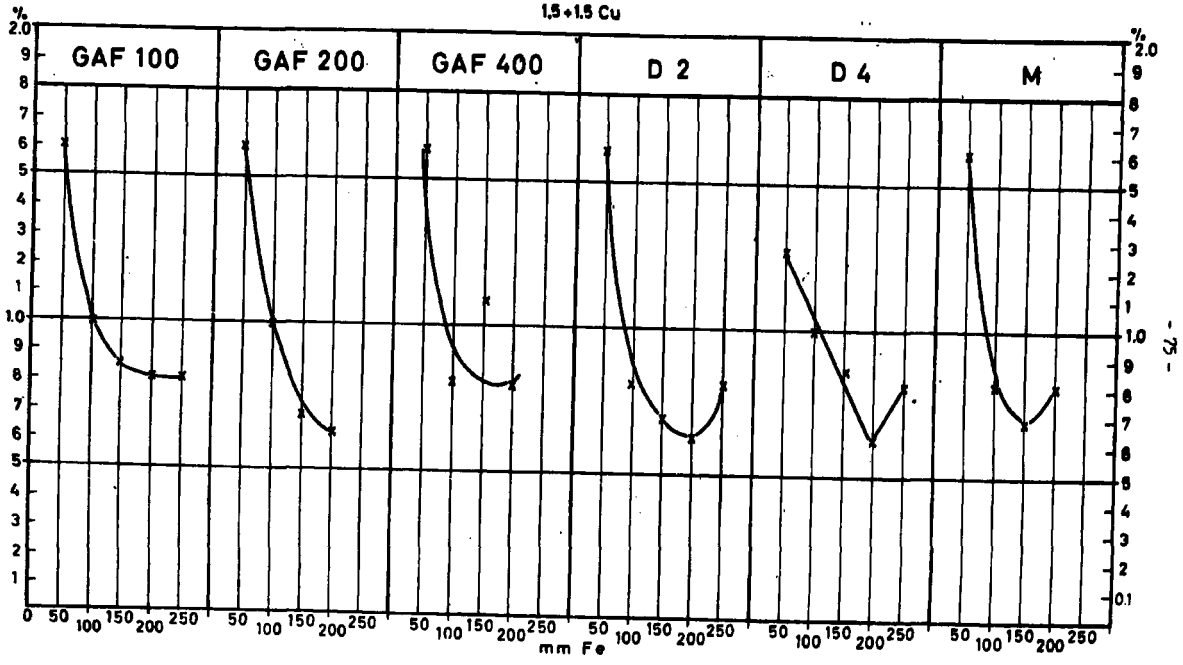

Fig.47. IQI sensitivities for 1.5 + 1.5 mm Cu screens

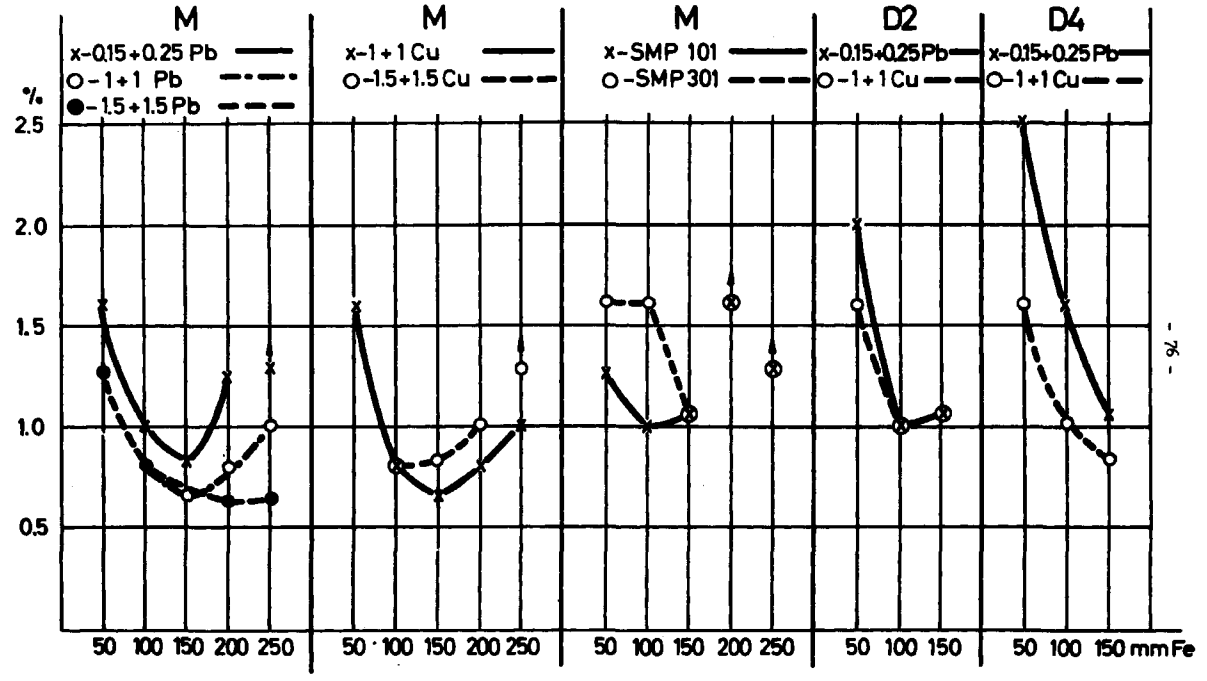

Fig.48 . IQI sensitivities for different film-screen combinations

Fig.49. Geometric unsharpness of the radiographic image

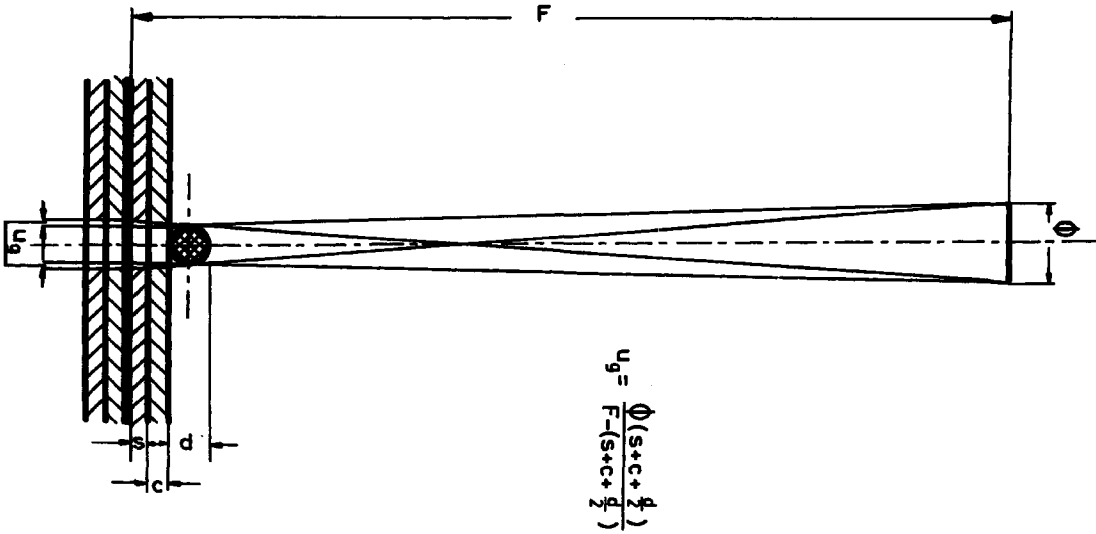

$$u_g = \frac{\Phi (s+c+\frac{d}{2})}{F-(s+c+\frac{d}{2})}$$

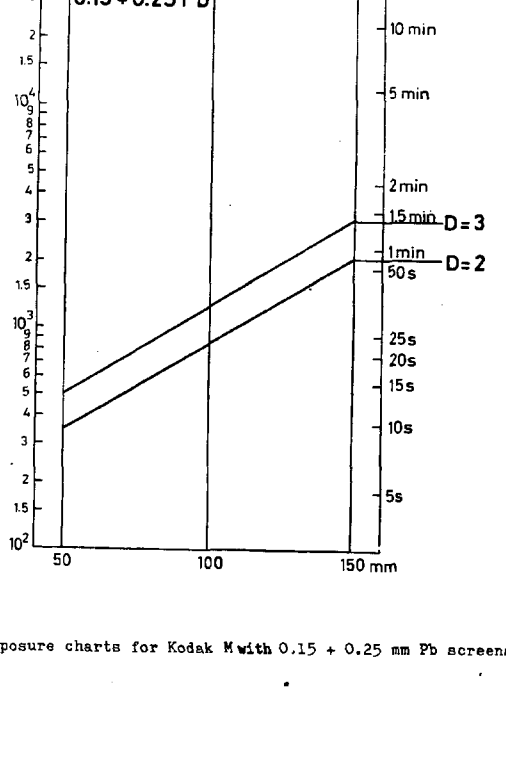

Fig.50. Exposure charts for Kodak M with 0.15 + 0.25 mm Pb screens

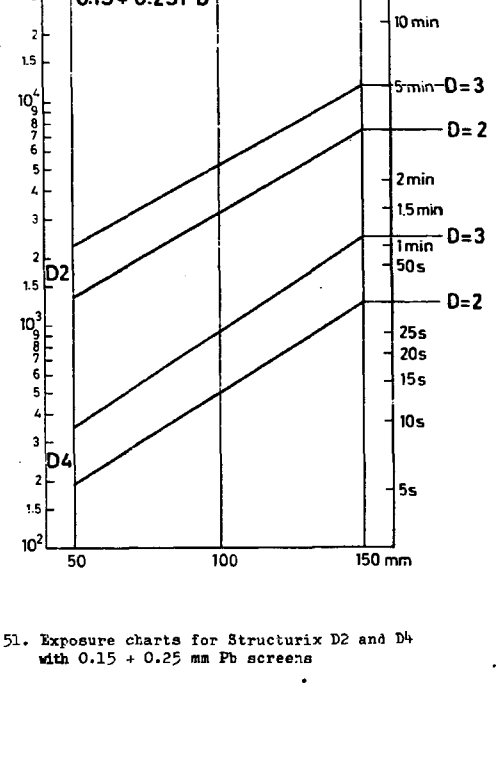

Fig.51. Exposure charts for Structurix D2 and D4 with 0.15 + 0.25 mm Pb screens

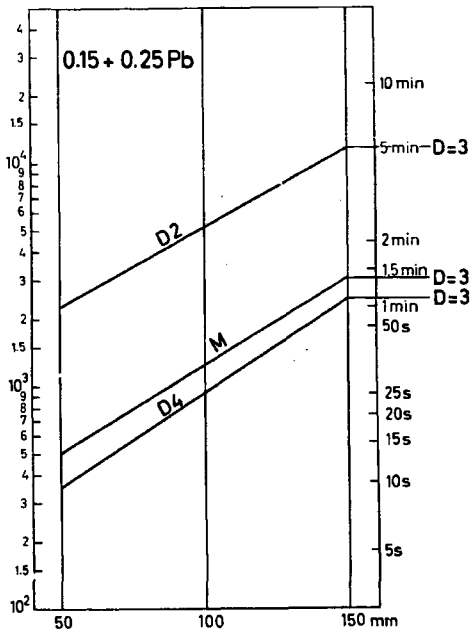

Fig. 52. Comparison of exposure charts from figs. 50 and 51

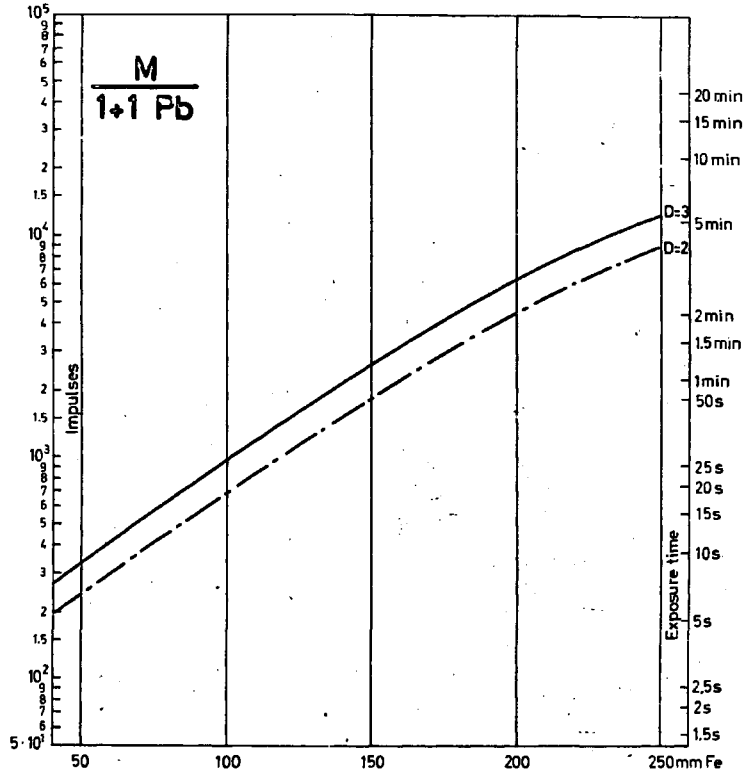

Fig.53. Exposure charts for Kodak M with 1 + 1 mm Pb screens

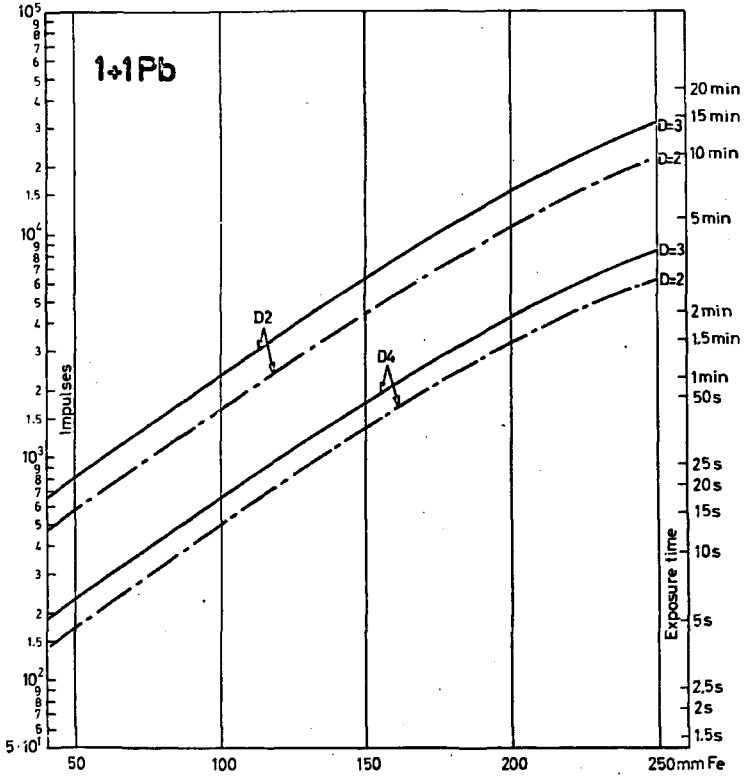

Fig.54. Exposure charts for Stucturix D2 and D4 with 1 + 1 mm Pb screens

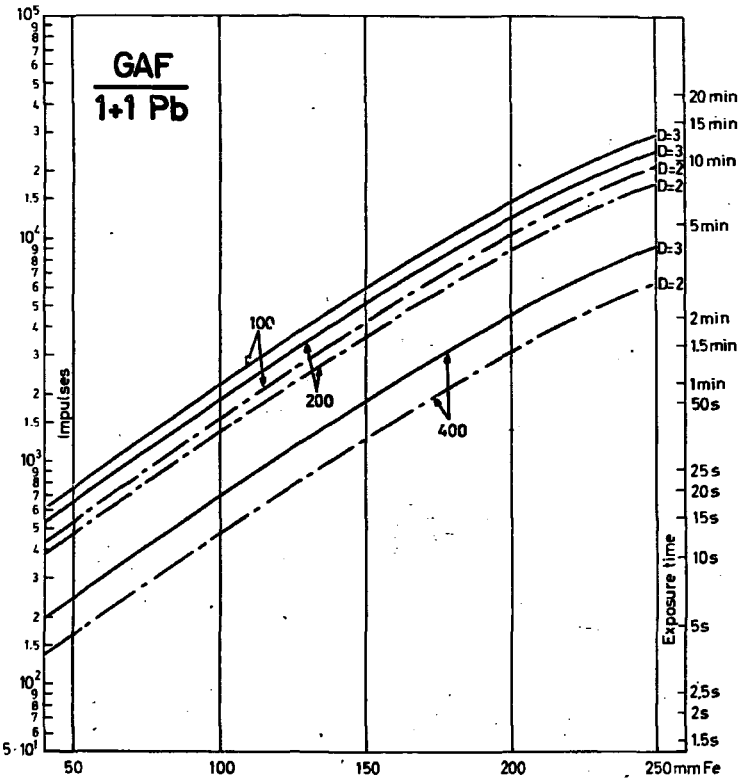

Fig.55. Exposure charts for GAF films with 1 + 1 mm Pb screens

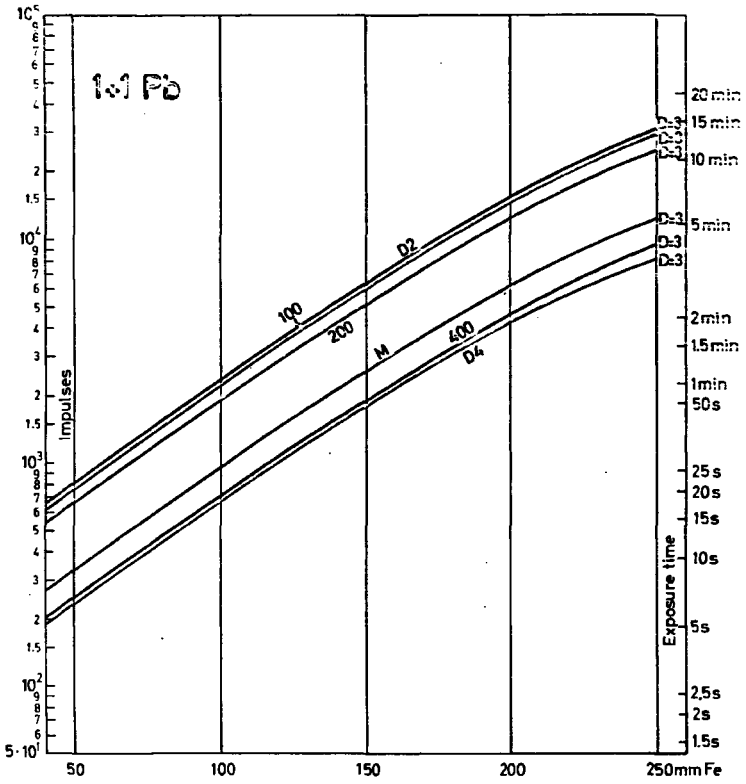

Fig.56. Comparison of exposure charts from figs. 53 to 55

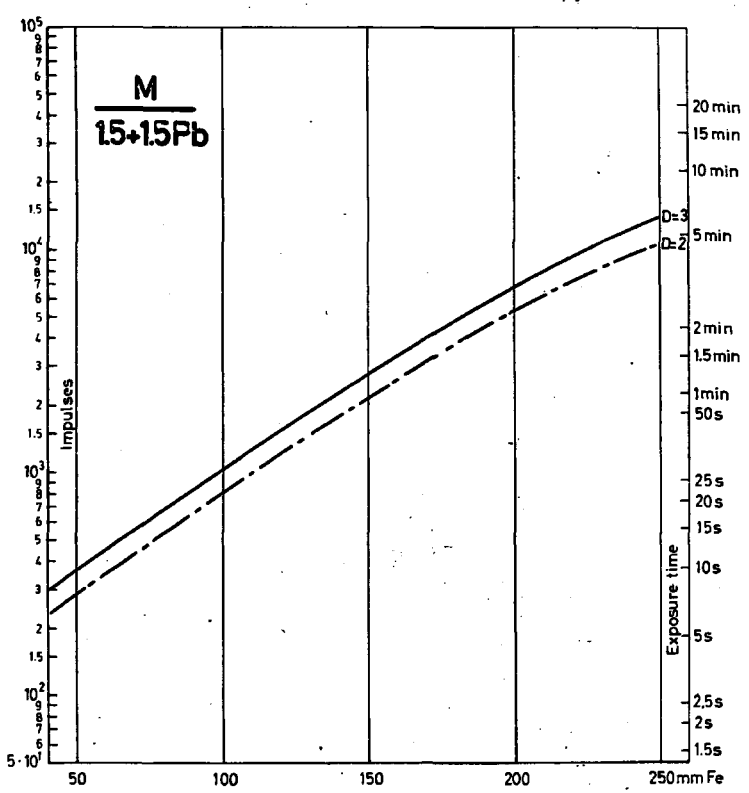

Fig.57. Exposure charts for Kodak M with 1.5 + 1.5 mm Pb screens

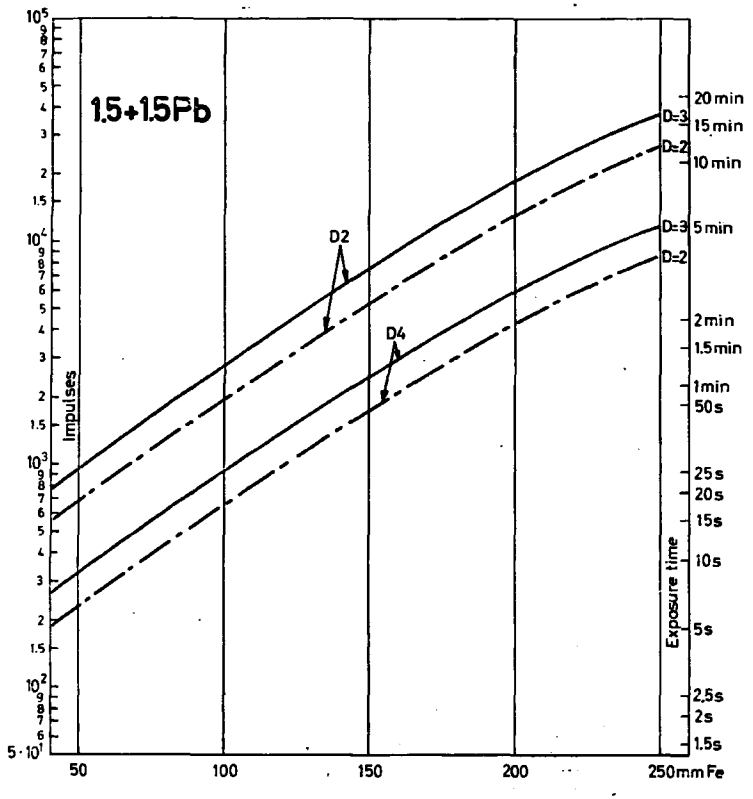

Fig.58. Exposure charts for Structurix D2 and D4 with 1.5 + 1.5 mm Pb screens

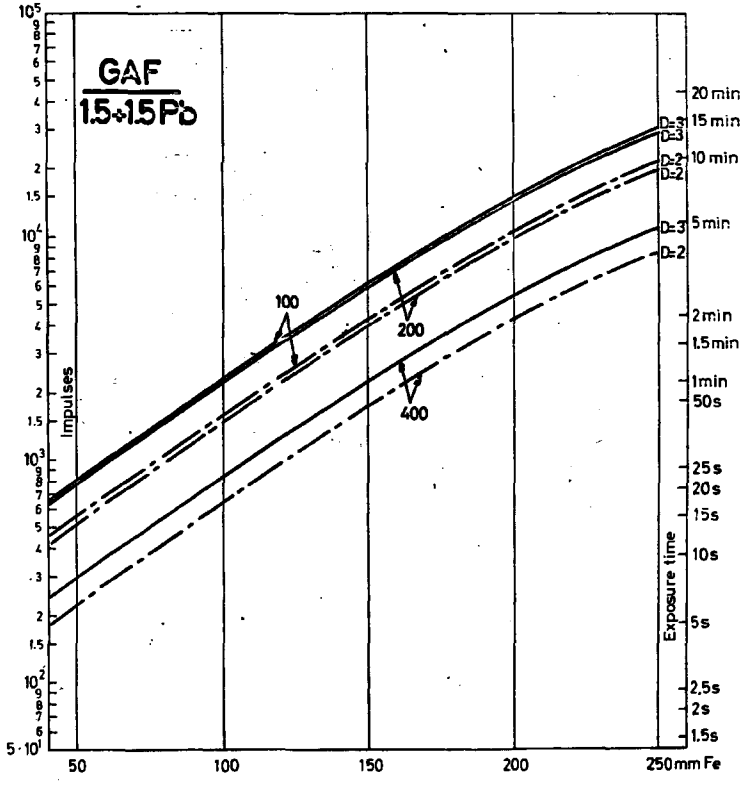

Fig.59. Exposure charts for GAF films with 1.5 + 1.5 mm Pb screens

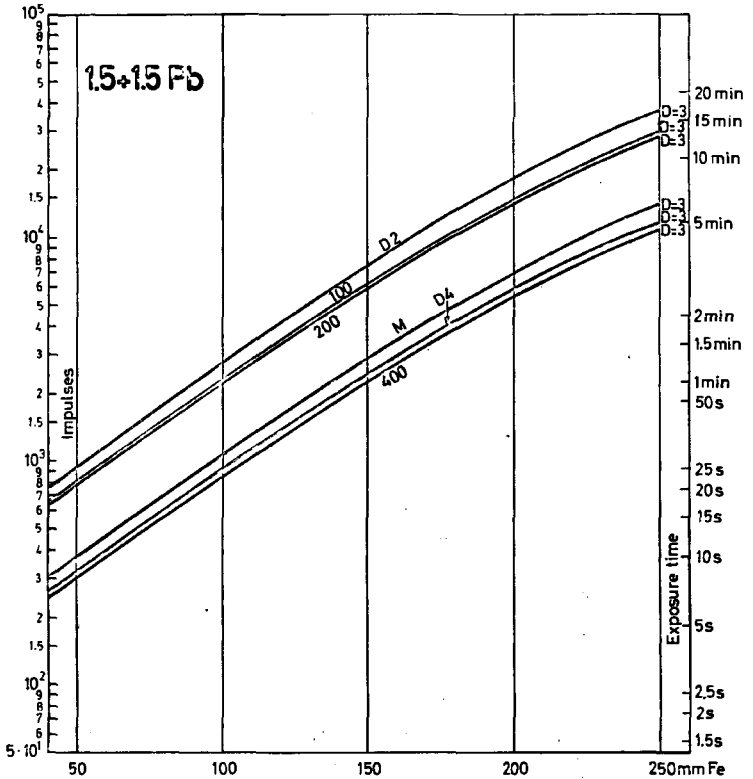

Fig.60. Comparison of exposure charts from figs.57 to 59

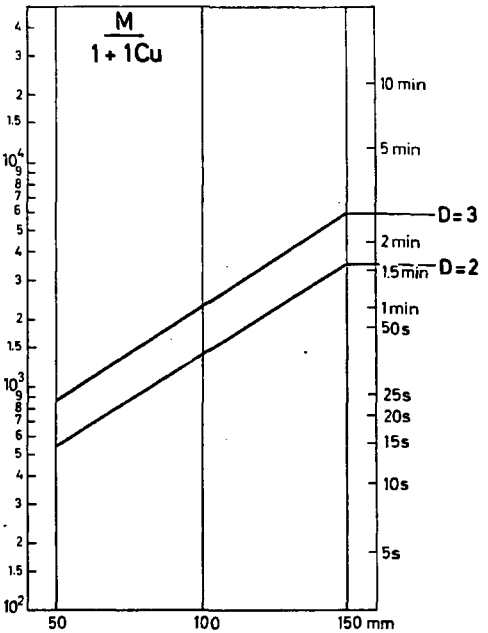

Fig.61. Exposure charts for Kodak M with 1 + 1 mm Cu screens

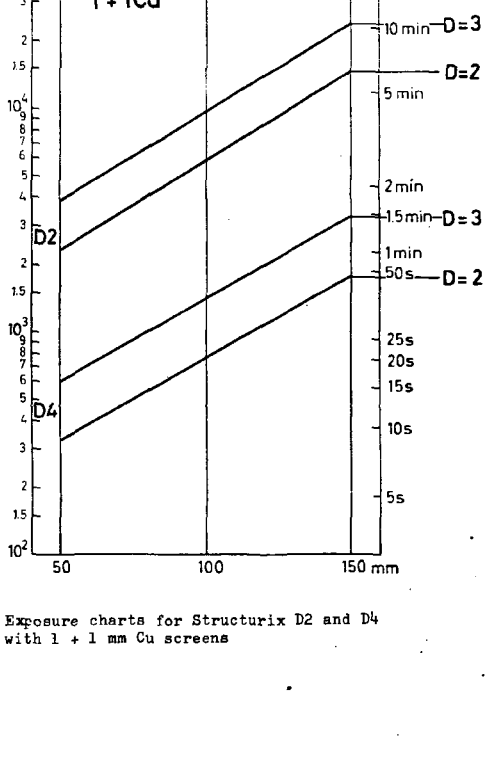

Fig.62. Exposure charts for Structurix D2 and D4 with 1 + 1 mm Cu screens

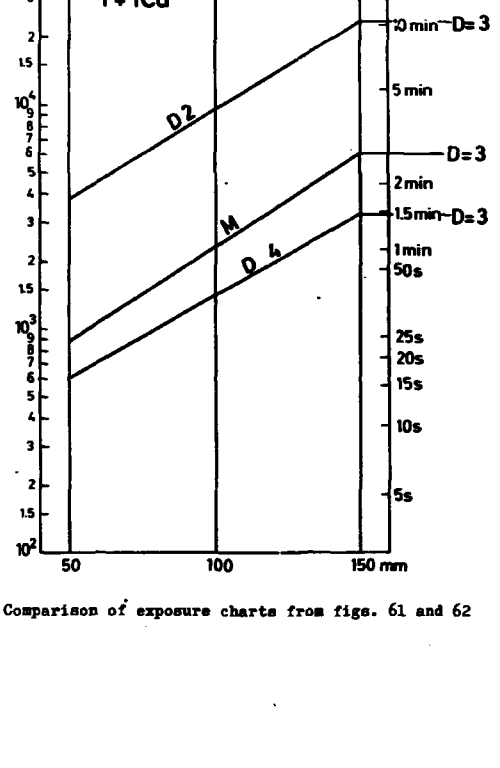

Fig.63. Comparison of exposure charts from figs. 61 and 62

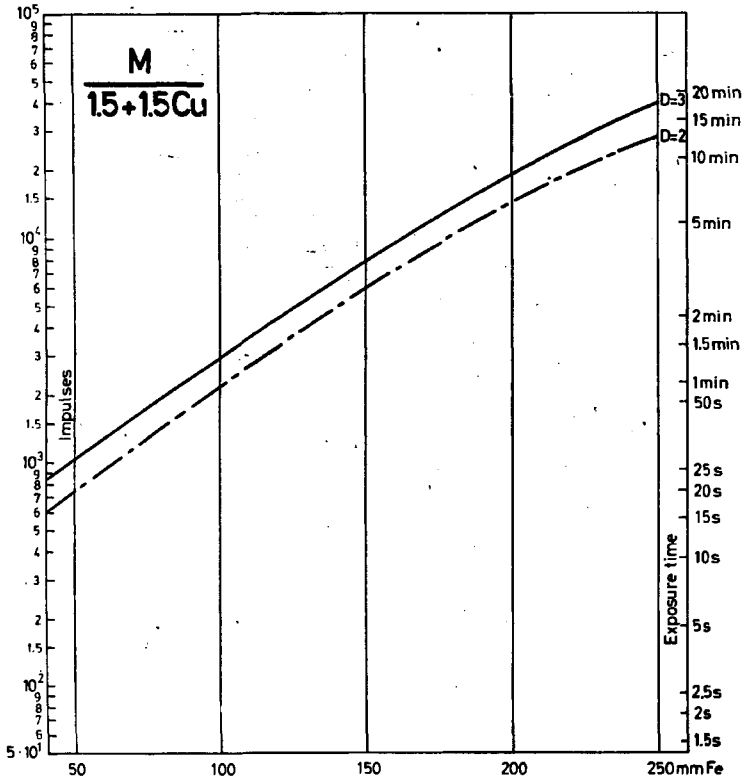

Fig.64. Exposure charts for Kodak M with 1.5 + 1.5 mm Cu screens

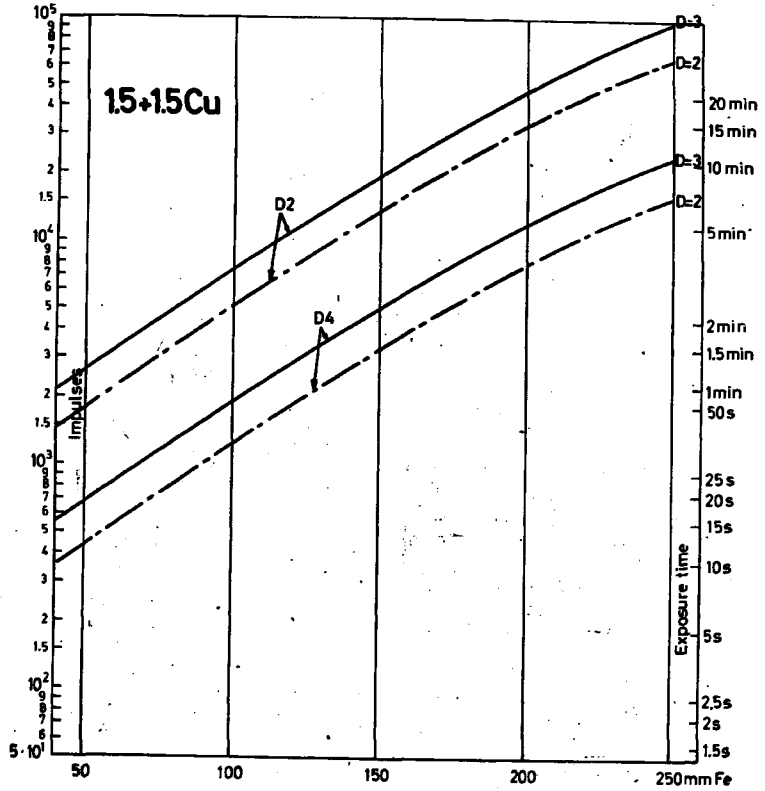

Fig. 65. Exposure charts for Structurix D2 and D4 with 1.5 + 1.5 mm Cu screens

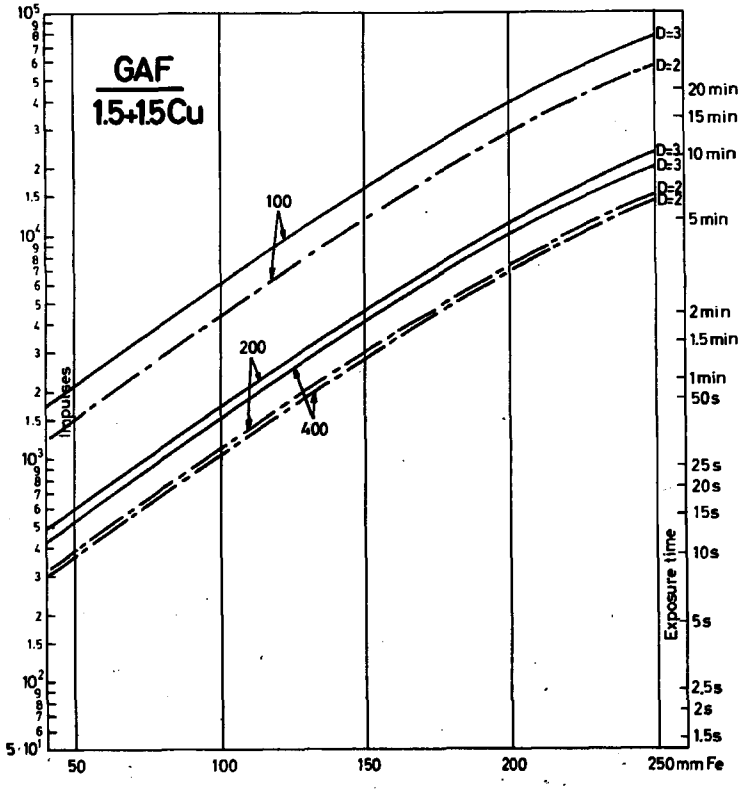

Fig.66. Exposure charts for GAF films with 1.5 + 1.5 mm Cu screens

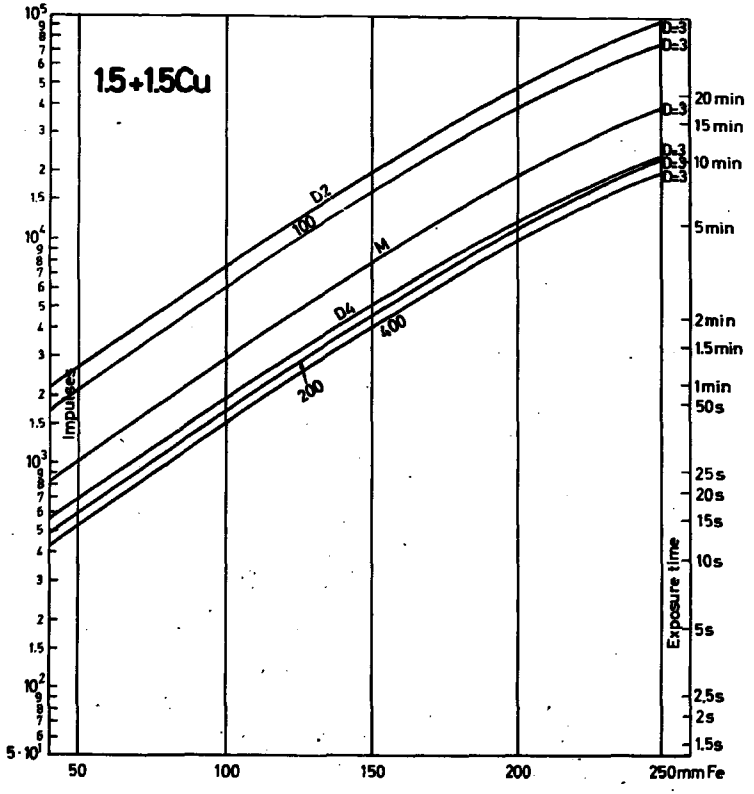

Fig.67. Comparison of exposure charts from figs. 64 to 66

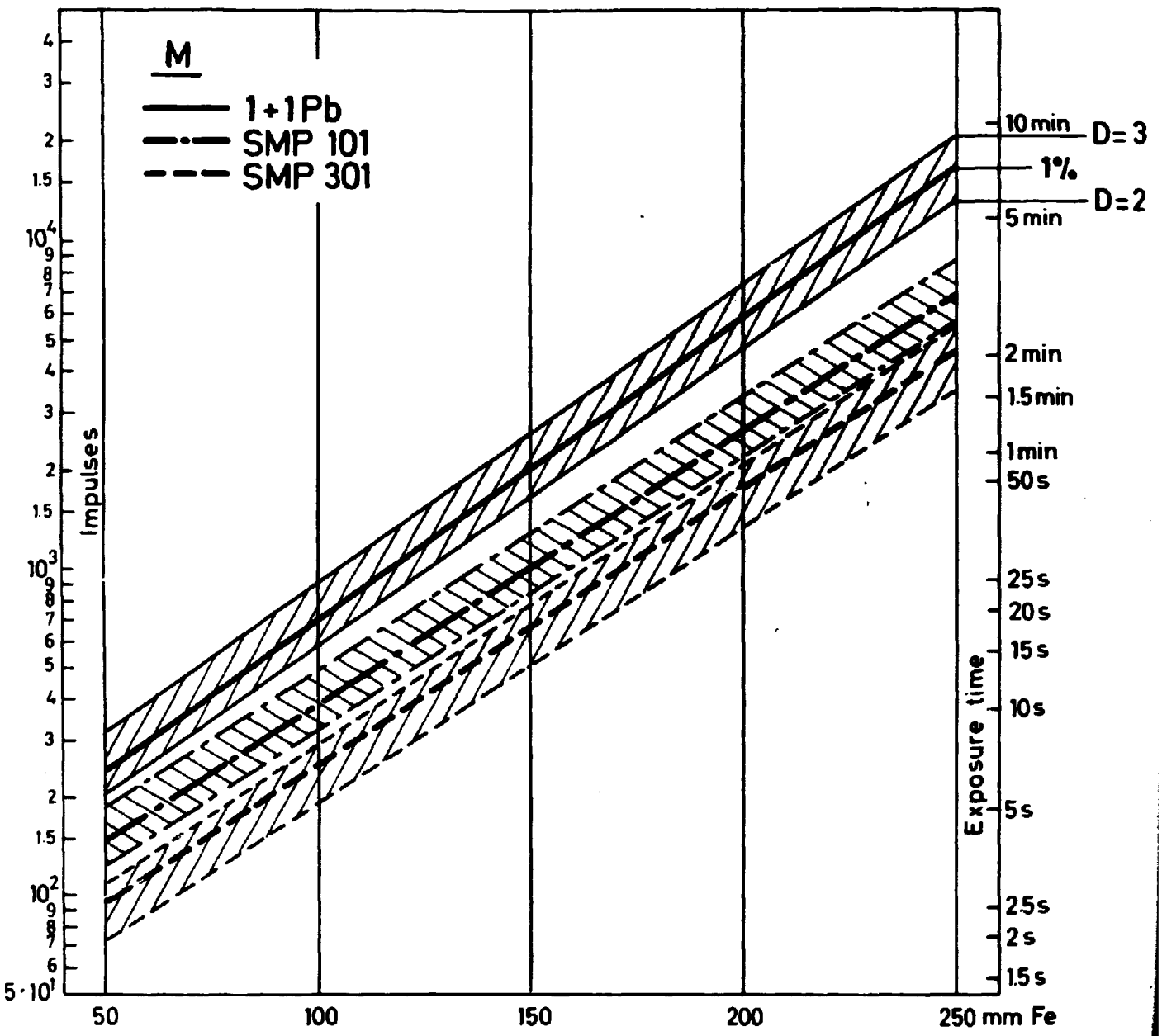

Fig.68. Exposure charts for Kodak M with 1 + 1 mm Pb and SMP 101 and SMP 301 screens